limited usefulness of cytokines for ex vivo expansion of CB HSCs. Thus, further improvement in ex vivo expansion procedures is necessary to prepare more efficient HSCs.

During the last few years, several molecules that can contribute to HSC self-renewal have been identified and characterized. These include external signaling molecules such as Wnt [7–10], bone morphogenic protein (BMP) [11], Sonic hedgehog (SHH) [12], and Notch ligands [13–15]. Furthermore, endogenous transcriptional modulators such as HOXB4 and Bmi-1 have been shown to be important for HSC self-renewal [16–18]. Among these, HOXB4 is of particular interest because it promotes prominent expansion of HSCs without causing leukemia. When HOXB4 was introduced into murine or human HSCs by gene transfer or protein delivery, these HSCs could be expanded without losing their normal potentials for differentiation into all lineages and for long-term repopulation, with a few exceptions [16, 19–22]. In addition to HOXB4, other HOX homeobox transcription factors play important roles in the proliferation and differentiation of hematopoietic cells [23, 24]. For example, HOXA9 regulates HSCs by mediating the expression of a variety of gene families [25, 26]. HOXA5/A10 and HOXB6 induce differentiation toward the myelomonocytic or erythroid lineage, respectively [27–30]. Furthermore, other HOX transcription factors, especially paralogous groups from A, B, and C, are expressed in normal hematopoietic cells; however, their physiological functions have not been elucidated.

HOX proteins have been demonstrated to interact with non-HOX homeobox family proteins (i.e., PBX and MEIS) at the DNA sequence 5′-TGATNNAT(G/A)(G/T)-3′ in the regulatory region of target genes [31, 32]. These protein complexes regulate target gene expression both positively and negatively, dependent on binding to coactivators or corepressors such as CBP/p300, histone deacetylases, or NcoR/SMRT [33–36]. For a subset of HOX proteins, the formation of a HOX-PBX-DNA ternary complex is mediated through both the HOX homeodomain and a short, conserved YPWM motif located just upstream of the HOX homeodomain [37, 38]. The interaction between the YPWM motif of HOX and the third α-helix in the homeodomain of PBX1 is thought to modify HOX-PBX1 DNA-binding affinity and transcriptional activity [39–41]. In addition, it was reported that PBX1 expressed in HSCs is a negative regulator of HOXB4-mediated self-renewal of HSCs [42]. Consistent with this report, a very recent study demonstrated that although DNA-binding activities are necessary for HOXB4 to expand HSCs ex vivo, the interaction with PBX1 is dispensable for this function [43].

In an attempt to expand potent CB HSCs with high efficiency, we synthesized a peptide containing the YPWM motif from HOX, which was predicted to modify HOX function by inhibiting binding between the YPWM motif in endogenous HOX and the PBX1 homeodomain. Here we show that this decoy HOX (decHOX) peptide augments the cytokine-dependent ex vivo expansion of CD34-positive hematopoietic stem/progenitor cells ($CD34^+$ hHSCs/HPCs), and these cells have the ability to reconstitute hematopoiesis more effectively and rapidly in mice that received transplants.

Materials and Methods

Peptide Synthesis

Peptides were synthesized at Greiner Bio-One (Tokyo, Japan, http://www.gbo.com/en) with purities of more than 95%. Synthetic peptides were lyophilized and stored at −20°C until use.

Reagents and Antibodies

Recombinant human SCF, TPO, IL-6, and sIL-6R were provided by Kirin Brewery (Tokyo, Japan, http://www.kirin.co.jp/english/). Recombinant human FL was purchased from R&D Systems Inc. (Minneapolis, http://www.rndsystems.com). Anti-asialo-GM1 antibody (Ab) was purchased from Wako Chemical (Osaka, Japan, http://www.wako-chem.co.jp/english). Antibodies (Abs) against HOXB4 (N-18) and PBX1 (P-20) were purchased from Santa Cruz Biotechnology Inc. (Santa Cruz, CA, http://www.scbt.com).

Plasmids

The expression vectors for HOXB4 and PBX1 were kindly provided by Dr. R. K. Humphries (British Columbia Cancer Agency, Vancouver, BC, Canada) and Dr. M. Featherstone (McGill University, Montreal, QC, Canada), respectively.

Preparation of Glutathione *S*-Transferase Fusion Proteins

Mutants of PBX1 were generated by polymerase chain reaction (PCR) and subcloned into pGEX-5X-1 (GE Healthcare Bio-science Corp., Piscataway, NJ, http://www.gehealthcare.com). Glutathione *S*-transferase (GST)-PBX1 fusion proteins were produced in *Escherichia coli* and purified as described previously [44].

In Vitro Binding Assays Using the BIAcore System

To assess in vitro binding between decHOX and PBX1, we used the BIAcore system (Biacore AB, Uppsala, Sweden, http://www.biacore.com/lifesciences/index.html). The details of this system are described elsewhere [45]. Briefly, we immobilized decHOX on the surface of CM5 sensor chips. Solution containing each GST-PBX1 fusion protein was injected over the sensor chips. Binding kinetics were monitored by changes in the weight of sensor chips and evaluated as arbitrary resonance units (RUs).

Mice

Nonobese diabetic/Shi-severe combined immunodeficient (NOD/SCID) mice, which lack mature lymphocytes and circulating complement proteins and have defective macrophages, were obtained from Jackson Laboratory (Bar Harbor, ME, http://www.jax.org). The mice were kept in microisolator cages on laminar flow racks in a clean experiment room and fed an irradiated, sterile diet and autoclaved, acidified water. Animal care was in accordance with institutional guidelines.

Cell Preparation

Human umbilical CB was obtained from normal, full-term deliveries upon obtaining informed consent. After sedimentation of the red blood cells with 6% hydroxyethyl starch (HES), mononuclear cells (MNCs) were separated by Ficoll-Hypaque density gradient centrifugation. $CD34^+$ cells were purified from MNCs using a MACS Direct CD34 Progenitor Cell Isolation Kit

(Miltenyi Biotec, Bergisch Gladbach, Germany, http://www.miltenyibiotec.com). After purification, over 95% of the separated cells were confirmed to be $CD34^+$ by flow cytometric analysis (data not shown). Each experiment was performed with cord blood $CD34^+$ cells derived from the same sample.

Suspension Cultures

Purified $CD34^+$ cells were seeded at a cell density of $1–2 \times 10^4$ cells per milliliter in 24-well tissue plates (Falcon, Becton, Dickinson and Company, Franklin Lakes, NJ, http://www.bd.com) with QBSF-60 serum-free medium (Quality Biological, Inc., Gaithersburg, MD, http://www.qualitybiological.com) containing SCF (100 ng/ml), FL (100 ng/ml), TPO (10 ng/ml), IL-6 (100 ng/ml), and sIL-6R (100 ng/ml). Cells were cultured in humidified air with 5% CO_2 at 37°C.

Protein Delivery

Synthetic peptides were delivered into 293T and CB $CD34^+$ cells using the Profect Protein Delivery System (Targeting Systems, Santee, CA, http://www.targetingsystems.com) according to the manufacturer's instructions.

Colony Assays

Cells were seeded into methylcellulose medium (MethoCult GF H4434V; Stem Cell Technologies, Vancouver, BC, Canada, http://www.stemcell.com) at a density of 2.5×10^2 cells per 35-mm dish and were cultured with 5% CO_2 at 37°C. All cultures were performed in triplicate, and the numbers of colonies were counted after 10 days.

Reconstitution Assays Using NOD/SCID Mice

Transplantation assays using NOD/SCID mice were performed according to procedures described previously [4] with some modifications. Briefly, 6–8-week-old NOD/SCID mice were total-body irradiated (TBI) with a dose of 2.4 Gy (60 Co) and then transplanted with the whole of peptide-treated cells or 2×10^4 freshly isolated $CD34^+$ cells through the tail vein. Because natural killer cell activity is retained in NOD/Shi-scid mice, the recipients were injected i.p. with 400 μl of phosphate-buffered saline containing 20 μl of anti-asialo-GM1 Ab immediately before cell transplantation. Identical treatments were performed on days 7 and 14. The proportion of reconstituted human cells in peripheral blood (PB) or bone marrow (BM) was assessed by flow cytometry with the anti-human CD45 Ab. For secondary transplantations, bone marrow cells were obtained from tibiae and femurs of the first mice that received transplants 12 weeks after transplantation, and 0.5×10^7 total bone marrow chimeric cells were injected into secondary NOD/SCID recipients subjected to immunosuppressive treatment before and after transplantation as described above ($n = 5$). Six weeks after transplantation, the presence of transplanted human cells in recipient BM was confirmed by flow cytometry as described above.

Limiting Dilution Analysis

The frequencies of human HSCs that were capable of repopulating in NOD/SCID mice in freshly isolated CB $CD34^+$ cells and peptide-treated cells were quantified by a limiting dilution analysis as described previously [46–48]. In this analysis, to avoid graft rejection, the recipients were treated with TBI in combination with anti-asialo-GM1 Ab immediately before and after transplantation (days 7, 14, 21, and 28). Data from several limiting dilution experiments were pooled and analyzed by applying Poisson statistics to the single-hit model. Frequencies were calculated using the maximum likelihood estimator.

Luciferase Assays

The details of the −1,137-c-*myc*-Luc vector, containing a 1,653-base pair (bp) fragment of the c-*myc* promoter (–1,137 to +516), were described previously [49]. To construct 3 × HB4(–316)-Luc and 3 × HB4(–72)-Luc, three tandem repeats of HOXB4-responsive elements at the indicated positions in the insulin-like growth factor-binding protein (IGFBP)-1 promoter were subcloned into pGL3 basic-TK-Luc. The sequences of the HOXB4-responsive elements were as follows: HB4(–316), 5′-CTTGTGTCAATTAAAGA and HB4(–72), 5′-GCGCTGCCCAATCATTAA. Luciferase assays were performed with a Dual-Luciferase Reporter System (Promega, Madison, WI, http://www.promega.com) as previously described [50]. Briefly, 293T cells (2×10^5 cells) were seeded in a 60-mm dish and cultured for 24 hours. Using the calcium phosphate coprecipitation method, cells were transfected with 6 μg of pcDNA3-HOXB4 alone or in combination with 6 μg of pCS2-PBX1a, along with 2 μg of reporter gene and 10 ng of pRL-CMV, a *Renilla* luciferase expression vector. After 12 hours, cells were washed, serum-starved for 24 hours, and subjected to luciferase assays. In some experiments, various doses of synthetic peptides were delivered into 293T cells 24 hours prior to luciferase assays.

Electrophoretic Mobility Shift Assay

Electrophoretic mobility shift assay (EMSA) was performed as previously described [51]. The double-stranded oligonucleotide HB4(–316) (described above) was used as a probe or competitor.

Semiquantitative Reverse Transcription PCR Analysis

Total RNA was isolated from 5×10^4 cells using a Concert Micro-to-Midi Total RNA Purification System (Invitrogen, Carlsbad, CA, http://www.invitrogen.com). Reverse transcription PCR (RT-PCR) was performed using a SuperScript One-Step RT-PCR system (Invitrogen) according to the manufacturer's instructions with forward/reverse primer sets as follows: c-myc, 5′-CTT CTG CTG GAG GCC ACA GCA AAC CTC CTC and 5′-CCA ACT CCG GGA TCT GGT CAC GCA GGG; $p21^{waf1/cip1}$, 5′-ACA GCA GAG GAA GAC CAT GT and 5′-GGT ATG TAC ATG AGG AGC TG; and β-actin, 5′-GGC GGC AAC ACC ATG TAC CCT and 5′-AGG GGC CGG ACT CGT CAT ACT.

Chromatin Immunoprecipitation Assays

Chromatin immunoprecipitation (ChIP) assays were performed with a ChIP Assay Kit (Upstate, Charlottesville, VA, http://www.upstate.com). Briefly, after transfection with various expression vectors, 293T cells were fixed with 1% formaldehyde. After isolation of nuclear extract, the chromatin was sonicated. Then, protein-DNA complexes were immunoprecipitated with 2 μg of anti-PBX1, anti-HOXB4, or anti-actin Ab. Immunoprecipitated DNA was eluted and subjected to PCR analysis with the following primer pair to amplify 420 bp of the human IGFBP-1 promoter (M59316): forward primer, 5′-GGC ATT

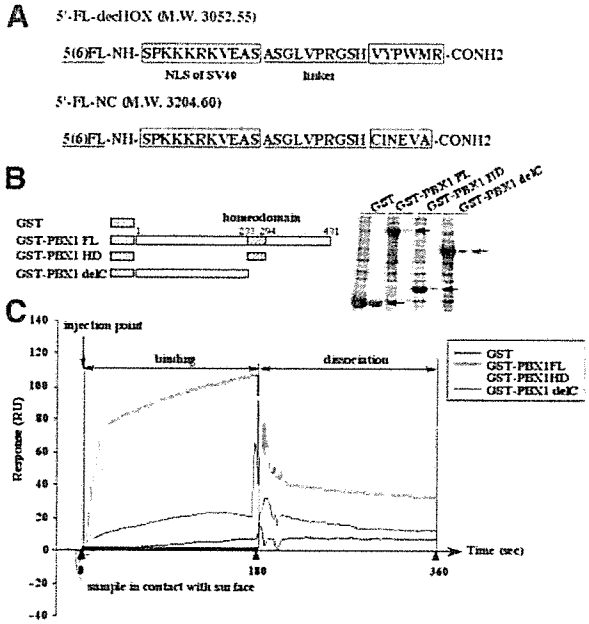

Figure 1. Binding of decHOX to GST-PBX1. **(A):** The structures of the 5′-FL synthetic peptides 5′-FL-decHOX and 5′-FL-NC are indicated. **(B):** GST-PBX1 fusion proteins expressed in *E. coli* were purified by glutathione-Sepharose 4B beads, and their qualities and quantities were confirmed by Coomassie staining. **(C):** In vitro binding of GST-PBX1 to decHOX evaluated by the BIAcore system, with decHOX attached to the sensor chip. To examine the kinetics of the binding and dissociation, various GST-PBX1 proteins were injected onto the sensor chip for 180 seconds and then washed with HEPES-buffered saline for 180 seconds. Abbreviations: decHOX, decoy HOX; delC, C-terminal deletion; FL, fluorescein; GST, glutathione *S*-transferase; HD, homeobox domain; M.W., molecular weight; NC, negative control; NH NLS, nuclear localization signal; RU, resonance unit.

GTT TTC TGC GTT TGA GAA CTG CTG; reverse primer, 5′-CTG GAC ACA GCG CGC ACC TTA TAA AGG GCA. After electrophoresis, PCR products were visualized with ethidium bromide staining.

Statistical Analysis

Data are presented as mean ± SEM or mean ± SD. The statistical significance of the data was determined by the Mann-Whitney *U* test or Student's *t* test. The significance level was set at .05.

Results

The Synthetic Peptide decHOX Binds Directly to the Homeodomain of PBX1

In this study, we attempted to expand CB CD34$^+$ hHSC/HPCs by modifying the function of HOX family proteins. For this purpose, we designed and synthesized a peptide designated decHOX, which was expected to inhibit the interaction between HOX and PBX1. decHOX contains the YPWM motif of HOX, used for its cooperative interaction with PBX1 [36, 37], and the nuclear localization signal (NLS) of the SV40 large T antigen (Fig. 1A) [52]. The negative control (NC) peptide contains the unrelated amino acid sequence CINEVA. To evaluate the efficiency of peptide delivery into CB CD34$^+$ hHSC/HPCs and the subsequent kinetics, FL protein was conjugated to the N termini of both peptides.

First, we examined in vitro binding between decHOX and several GST-PBX1 fusion proteins using the BIAcore system. In this system, the analyte protein is injected onto the sensor chip, the surface of which is covered by the immobilized partner ligand. Binding of the ligand to the analyte is monitored by an increase in arbitrary RUs. Prior to this analysis, we purified several GST-PBX1 fusion proteins (Fig. 1B, left panel) and confirmed their qualities and quantities by Coomassie Brilliant Blue staining (Fig. 1B, right panel). Injection of either GST-full-length PBX1 protein (GST-PBX1 FL) or GST-PBX1 homeobox domain (HD) protein (GST-PBX1 HD) over the decHOX surface resulted in a significant increase in RUs with a lapse of 3 minutes for the binding reaction (Fig. 1C), and these signals increased in a dose-dependent manner (data not shown). In contrast, GST alone and GST-PBX1 delC (lacking the HD) did not bind appreciably to decHOX. After the binding reaction, we injected HEPES-buffered saline for 180 seconds. During this dissociation reaction, GST-PBX1 HD bound to decHOX more stably than GST-PBX1 FL (Fig. 1C). These results suggest that GST-PBX1 FL and GST-PBX1 HD bind to decHOX, probably through HD.

decHOX Can Modulate the Transcriptional Activity of HOX-PBX

To assess the effects of decHOX on HOX-PBX-mediated gene expression, we performed luciferase assays with three types of reporter genes for HOXB4, one containing the c-*myc* promoter (–1,137-c-*myc*-Luc) and the other two containing IGFBP-1 promoters (3 × HB4[–316]-Luc and 3 × HB4[–72]-Luc) as responsive elements, as described previously [49, 53]. Although HOXB4 activated –1,137-c-*myc*-Luc 5.2-fold in 293T cells, PBX1 suppressed this induction (Fig. 2B). However, this inhibitory effect of PBX1 was decreased in a dose-dependent manner by pretreatment with decHOX. Similar responses were observed in assays using 3 × HB4(–316)-Luc and 3 × HB4(–72)-Luc (Fig. 2B). These results indicate that decHOX can enhance the activity of HOXB4 that is suppressed by PBX1.

In a previous study using EMSA, mutant HOX proteins that cannot bind to PBX1 were shown to have defects in DNA-binding activities [39–41]. In contrast, it was reported that the interaction with PBX1 is not necessary for HOXB4 to induce HSC self-renewal [43]. Because decHOX was designed to inhibit the interaction between HOX and PBX1, we evaluated the effect of decHOX on the DNA-binding activity of HOXB4-PBX1 using EMSA. For this purpose, we transfected 293T cells with wild-type (WT) HOXB4 or mutant HOXB4 harboring a WM→AA mutation in the YPWM motif (designated HOXB4 AA; Fig. 2C). Protein(s) in nuclear extracts from 293T cells transfected with PBX1 and HOXB4 WT bound to the HB4(–316) probe (Fig. 2C, lane 2). This band was abolished by WT DNA competitor (Fig. 2C, lane 3) but not by mutant (mt) competitor (Fig. 2C, lane 4), implying that it contains the HOXB4 WT-PBX1 complex. In contrast, proteins in the nuclear extract from HOXB4 AA-transfected cells scarcely bound to the probe, indicating the importance of the YPWM motif for the DNA-binding activity of HOXB4-PBX1 (Fig. 2C, lane 5). Also, pretreatment with decHOX inhibited DNA binding of the HOXB4 WT-PBX1 complex in a dose-

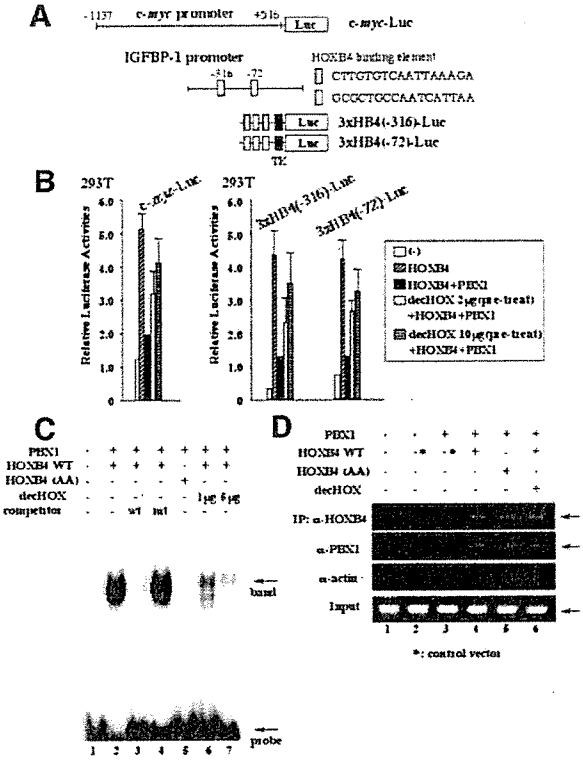

Figure 2. Effects of decHOX on DNA-binding and transcriptional activities of the HOX/PBX complex. **(A):** To construct –1,137-c-*myc*-Luc, a 1,653-base pair fragment of the c-*myc* promoter (–1137 to +516) was subcloned into the plasmid pSP72-Luciferase [47]. To generate 3 × HB4(–316)-Luc and 3 × HB4(–72)-Luc, three tandem repeats of HOXB4-responsive elements in the IGFBP-1 promoter at the indicated locations were subcloned into TK-pGL3 basic-Luc at just upstream of the murine minimal TK promoter linked to the firefly luciferase gene, and their sequences were as indicated. **(B):** 293T cells (2×10^5 cells) seeded in a 60-mm dish were transfected with 6 μg of pcDNA3-HOXB4 alone or in combination with 6 μg of pCS2-PBX1a along with 2 μg of reporter gene and 10 ng of pRL-CMV. After 12 hours, cells were washed, serum-starved for 24 hours, and subjected to luciferase assays using a Dual Luciferase Reporter Assay System. In some experiments, various doses of synthetic peptides were delivered into 293T cells 24 hours prior to luciferase assays. Results are shown as mean ± SD of triplicate cultures. **(C):** 293T cells were transfected with PBX1 together with HOXB4 WT or HOXB4 AA. After 36 hours, nuclear extract was isolated and subjected to electrophoretic mobility shift assay (EMSA) with probes of 3 × HB4(–316). In competition assays, a 200-fold excess of unlabeled wt or mt competitor oligonucleotide was added to the binding mixture. In some experiments, various doses of synthetic peptides were delivered into 293T cells 24 hours prior to EMSA. **(D):** 293T cells transfected with the indicated expression vectors were fixed with 1% formaldehyde. After the isolation of the nuclear extract, chromatin was sonicated. Then, protein-DNA-binding complexes were immunoprecipitated with the 2 μg of the indicated antibodies. Immunoprecipitated DNA was subjected to polymerase chain reaction (PCR) analysis with a primer pair that amplifies 420 base pairs of the human IGFBP-1 promoter. PCR products were electrophoresed onto the agarose gel and visualized with ethidium bromide staining. Abbreviations: decHOX, decoy HOX; IGFBP-1, insulin-like growth factor-binding protein; IP, immunoprecipitation; mt, mutant; WT, wild type.

dependent manner (Fig. 2C, Lanes 6 and 7). These results suggest that decHOX inhibits the interaction between HOXB4 and PBX1 in the ex vivo EMSA binding experiment, thereby suppressing the DNA-binding activity of the HOXB4 WT-PBX1 complex. However, in ChIP assays, which reflect the in vivo DNA-binding state of transcription factors more precisely than EMSA, the HOXB4 AA-PBX1 complex bound to the endogenous IGFBP-1 promoter as efficiently as the HOXB4 WT-PBX1 complex (Fig. 2D, top and second panels, lane 4 vs. lane 5). Also, decHOX barely influenced the DNA-binding activity of the HOXB4 WT-PBX1 complex (Fig. 2D, top and second panels, lane 4 vs. lane 6). Furthermore, we obtained similar results from ChIP assays using two additional primer sets that amplify different sites in the IGFBP-1 promoter (data not shown). From these results, we speculated that HOXB4 is capable of binding to DNA regardless of its interaction with PBX1. However, since we found that PBX1 bound to target DNA in the presence of HOXB4 AA, it is also possible that the YPWM is not required for the interaction between HOXB4 and PBX1. Because the latter speculation is inconsistent with several previous reports indicating the essential role of the YPWM motif in the interaction between HOXB4 and PBX1 [37, 38], further studies using several endogenous promoter sequences will be required to draw a definite conclusion.

decHOX Is Efficiently Delivered into CB CD34$^+$ and Colocalizes with PBX1

Next, we introduced 5′-FL-decHOX into CB CD34$^+$ hHSC/HPCs and analyzed the efficiency of delivery by examining fluorescein intensity with flow cytometry. CD34$^+$ hHSC/HPCs were isolated from CB using AutoMACS and cultured in QBSF-60 serum-free medium containing SCF, FL, TPO, IL-6, and sIL-6R. After culturing for 24 hours, FL-decHOX or FL-NC was delivered into CD34$^+$ cells using the Profect Protein Delivery System. Immediately after delivery (day 0; total culture day 2), 76.2% of CB CD34$^+$ cells were fluorescein-positive (Fig. 3A). Fluorescein intensity decreased with time in culture and was scarcely detectable at day 7. This result suggested that the direct influence of decHOX on CD34$^+$ hHSC/HPCs is limited to 7 days.

Next, we examined the subcellular localizations of PBX1, decHOX, and the NC peptide in hHSC/HPCs using fluorescent microscopy. Forty-eight hours after peptide delivery, both peptides were predominantly detected in the nucleus because of the respective nuclear localization signals. In NC-delivered cells, PBX1 was mainly localized in the cytosol (Fig. 3B, upper panel). On the other hand, in decHOX-delivered cells, PBX1 colocalized with decHOX in the nucleus (Fig. 3B, lower panel). These results suggested that decHOX could interact with PBX1 and colocalized with PBX1 in the nucleus.

decHOX Can Modulate HOX/PBX-Mediated Gene Expression in CB hHSC/HPCs

PBX1 is known to modulate the function of HOX proteins both positively and negatively [30, 32, 33]. For example, HOXB4 induces the expression of c-*myc* in HSCs, and this effect is suppressed by PBX1. On the other hand, HOXA10-mediated expression of $p21^{waf1/cip1}$ is enhanced by PBX1 in myelomonocytic progenitors [28]. To assess the effects of decHOX on the function of HOX proteins in CB cells, we examined the expression of these two target genes. First, to characterize CD34$^+$CD38$^+$ and CD34$^+$CD38$^-$ cells after the ex vivo expansion, we sorted these cells after 9 days in culture and

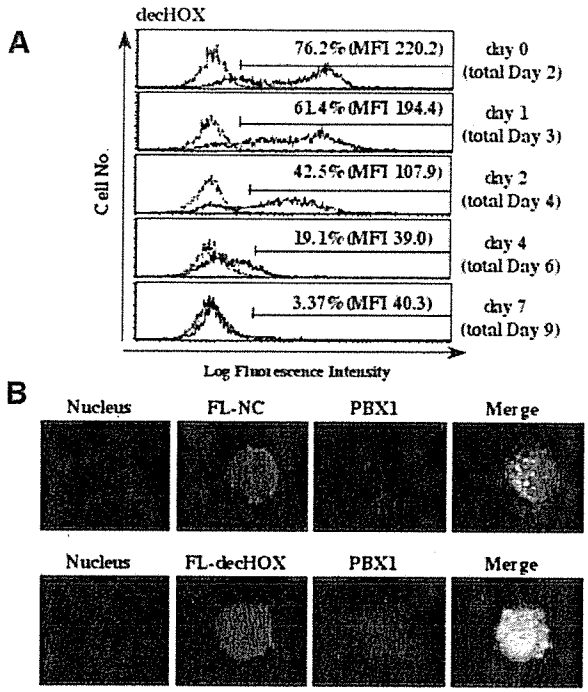

Figure 3. Expression and intracellular localization of decHOX in hHSC/HPCs. **(A):** FL-decHOX was transferred into $CD34^+$ cells by the Profect Protein Delivery System, and fluorescence intensity was assessed by flow cytometry at the indicated times. **(B):** Cytospin preparations of the FL-NC (upper panel)- or FL-decHOX (lower panel)-delivered $CD34^+$ cells were fixed, permeabilized, and incubated with a rabbit anti-human PBX1 antibody (Ab) for 1 hour and then with the anti-rabbit IgG Ab AlexaFluor 546. Cells were rinsed with phosphate-buffered saline containing Hoechst 33342. The stained cells were observed under a confocal laser microscope. Abbreviations: decHOX, decoy HOX; MFI, mean fluorescence intensity; NC, negative control.

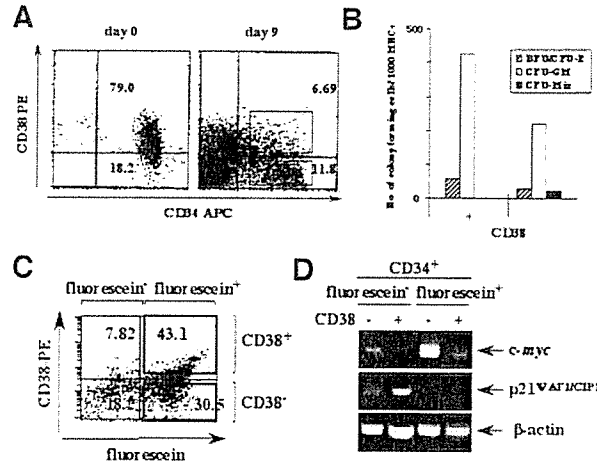

Figure 4. Effects of decoy HOX (decHOX) on target gene expression in hHSC/HPCs. Cord blood (CB) $CD34^+$ cells were cultured in QBSF-60 serum-free medium containing cytokines (stem cell factor, 100 ng/ml; fluorescein [FL], 100 ng/ml; TPO, 10 ng/ml; IL-6, 100 ng/ml; and sIL-6R, 100 ng/ml) for 9 days. **(A):** Before and after culturing, the expression of CD34 and CD38 were examined by flow cytometry. **(B):** After culturing, $CD34^+CD38^-$ and $CD34^+CD38^+$ cells were sorted and subjected to colony assays. **(C):** CB $CD34^+$ cells were treated with FL-decHOX for 48 hours, and then CD38 and fluorescein expression was examined by flow cytometry. **(D):** Cells from each fraction were sorted and subjected to RT-PCR analysis. Abbreviations: APC, allophycocyanin; CFU-GM, colony-forming unit-granulocyte/monocyte precursor; CFU-mix, mixed hematopoietic colony-forming unit.

performed methylcellulose colony assays (Fig. 4A). It was reported that $CD34^+CD38^-$ cells can develop from $CD34^+CD38^+$ cells through the loss of CD38 expression during culturing with cytokines [54]. We found that the primitive colony, mixed hematopoietic colony-forming unit (CFU-Mix) was formed from $CD34^+CD38^-$ cells but not from $CD34^+CD38^+$ cells. Therefore, we supposed that $CD34^+CD38^-$ cells were more primitive than the $CD34^+CD38^+$ cells that developed after ex vivo culturing. Next, we treated CB $CD34^+$ cells with 5′-FL-decHOX, cultured for 48 hours, and subjected them to flow cytometric analysis. At that point, 43.1% of the cultured cells were $fluorescein^+CD38^+$, 30.5% were $fluorescein^+CD38^-$, 7.82% were $fluorescein^-CD38^+$, and 18.2% were $fluorescein^-CD38^-$ (Fig. 4C). Then, we sorted the cells from each fraction and subjected them to semiquantitative RT-PCR analysis. In the $CD34^+CD38^-$ immature cell fraction, c-*myc* expression was increased in the decHOX-delivered $fluorescein^+$ fraction compared with the $fluorescein^-$ control fraction (Fig. 4D, top panel, lane 1 vs. lane 3). Conversely, in the $CD34^+CD38^+$ mature fraction, the expression of $p21^{waf1/cip1}$ was decreased in the $fluorescein^+$ fraction compared with the $fluorescein^-$ fraction (Fig. 4D, middle panel, lane 2 vs. lane 4). Together, these results suggest that decHOX binds to PBX1 as a HOX decoy and cancels both the positive and negative effects of PBX1 on HOX proteins in $CD34^+$ hHSC/HPCs.

decHOX Enhances Cytokine-Dependent Ex Vivo Expansion of CB hHSC/HPCs

Next, we examined effects of decHOX on the growth and differentiation of CB $CD34^+$ hHSC/HPCs. As shown in Figure 5, purified $CD34^+$ cells were exposed to 5′-FL-decHOX or 5′-FL-NC for 24 hours. Then, 1×10^4 $fluorescein^+$ cells were sorted and cultured in QBSF-60 serum-free medium containing SCF, FL, TPO, IL-6, and sIL-6R for 7 days, during which, medium dilution was performed as indicated. After these cultures, no apparent difference was observed between the total number of viable decHOX-treated and NC-treated cells (Fig. 6A). However, the proportion of $CD34^+$ cells was significantly higher in decHOX-treated cells than in NC-treated cells (decHOX, 33.2%; NC, 17.9%) (Fig. 6B). Similar results were obtained from five independent experiments (data not shown). Accordingly, the fold expansion of $CD34^+$ cells was higher in decHOX-delivered cells than in NC-delivered cells (decHOX, 32.5 ± 8.71-fold; NC, 17.2 ± 6.25-fold [$n = 6$] [$p < .05$]) (Fig. 6A). Furthermore, cultures treated with decHOX retained immature cells with $CD34^+CD38^-$ or $CD45^+HLA\text{-}DR^-$ phenotype more effectively than NC-treated cells (percentage $CD34^+CD38^-$ cells: decHOX, $24.2\% \pm 6.67\%$; NC, $14.8\% \pm 6.17\%$ [$n = 3$] [$p < .05$]; percentage $CD45^+HLA\text{-}DR^-$ cells: decHOX, $37.2\% \pm 6.98\%$; NC, $18.8\% \pm 7.44\%$ [$n = 3$] [$p < .05$]) (representative results from one experiment are shown in Fig. 6B). To characterize the ex vivo expanded cells, we ana-

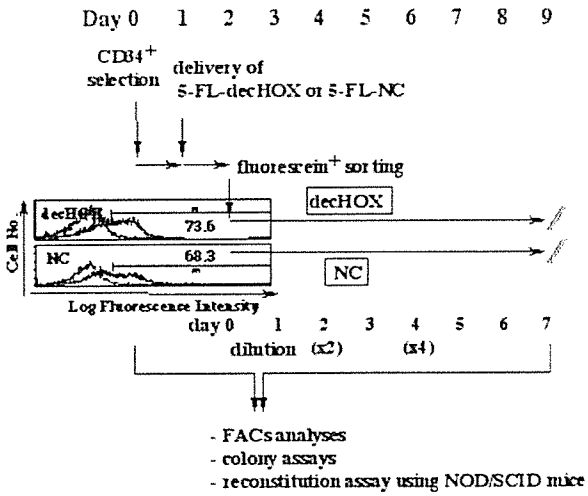

Figure 5. Experimental design. $CD34^+$ hematopoietic stem/progenitor cells were isolated from cord blood and cultured in serum-free medium containing cytokines. FL-decHOX or FL-NC was then delivered into $CD34^+$ cells. Twenty-four hours after peptide delivery, approximately 70% of cultured cells were fluorescein-positive. Fluorescein-positive cells were sorted and cultured for 7 days. Medium dilutions were performed as indicated. Cultured cells were then subjected to FACS analyses, colony assays, and reconstitution assays using NOD/SCID mice. Abbreviations: decHOX, decoy HOX; FACS, fluorescence-activated cell sorting; FL, fluorescein; NC, negative control.

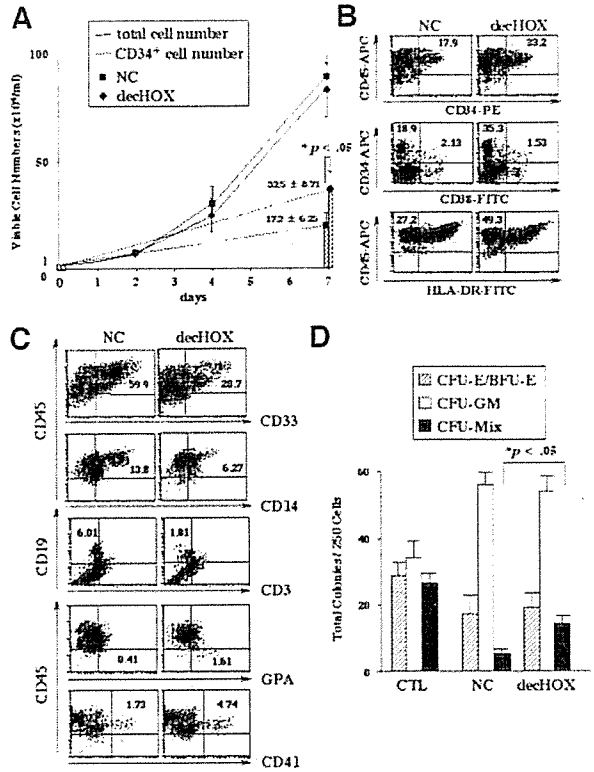

Figure 6. Effects of decHOX on biological properties and functions of hHSC/HPCs cultured with cytokines. After treatment with fluorescein (FL)-decHOX or FL-NC, fluorescein-positive cells were sorted and cultured for 7 days. **(A):** The total number of viable cells and their surface phenotypes were examined. Results are shown as mean ± SD ($n = 6$). **(B, C):** Representative fluorescence-activated cell sorting data from one experiment are shown. **(D):** Cultured cells were subjected to methylcellulose colony assays using freshly isolated cells as a control. All cultures were done in triplicate and scored after 10 days. Results are shown as mean ± SD ($n = 4$). Abbreviations: BFU-E, burst-forming unit-erythroid precursor; CFU-E, colony-forming unit-erythrocyte precursor; CFU-GM, colony-forming unit-granulocyte/monocyte precursor; CFU-Mix, mixed hematopoietic colony-forming unit; CTL, control; decHOX, decoy HOX; FITC, fluorescein isothiocyanate; HLA, human leukocyte antigen; NC, negative control; PE, phycoerythrin.

lyzed the expression of lineage markers on these cells (Fig. 6C). Fluorescence-activated cell sorting analyses after 7 days in culture indicated that both NC- and decHOX-treated cells contained not only immature cells but also mature cells expressing lineage markers such as CD33 (myeloid), CD14 (monocytic), CD19 (B lymphoid), GPA (erythroid), and CD41 (megakaryocytic). Except for GPA and CD41 expression, the expression of these markers was notably lower in decHOX-delivered cells than in NC-delivered cells. Next, we analyzed the effects of decHOX on colony-forming activities of CB $CD34^+$ hHSC/HPCs. As shown in Figure 6D, both decHOX- and NC-delivered cells, which contain approximately 33% and 18% of $CD34^+$ cells, respectively (Fig. 6B), generated all types of colonies, and the numbers of colony-forming unit-erythrocyte precursor/burst-forming unit-erythroid precursor and colony-forming unit-granulocyte/monocyte precursor colonies were nearly the same in both cultures. However, decHOX more effectively yielded CFU-Mix primitive colonies than NC (CFU-Mix colonies per 250 cultured cells: decHOX, 15.3 ± 2.1; NC, 7.5 ± 0.8 [$n = 6$] [$p < .05$]). Together, these results suggest that although both immature progenitors and mature cells were amplified during culturing, decHOX selectively expands immature progenitors.

decHOX-Treated hHSC/HPCs Reconstitute Hematopoiesis Rapidly and Efficiently in NOD/SCID Mice

Next, we assessed the effects of decHOX on engrafting abilities of CB $CD34^+$ hHSC/HPCs by xenotransplantation into NOD/SCID mice. For this purpose, 2×10^4 CB $CD34^+$ cells were treated with decHOX or NC and cultured in QBSF-60 containing cytokines for 7 days. Then, total cultured cells were transplanted into NOD/SCID mice that were treated with 2.4 Gy of TBI and i.p. injection of anti-asialo-GM1 Ab immediately before and after transplantation (days 7 and 14) (each group, $n = 9$). Also, 2×10^4 freshly isolated CB $CD34^+$ cells derived from the same sample as the expanded cells were transplanted as a control (CTL). CTL cells are expected to contribute to hematopoiesis in approximately 10% of BM cells after 4 weeks under our experimental conditions using NOD/SCID mice. When decHOX-treated cells were transplanted, human $CD45^+$ ($hCD45^+$) cells constituted 9.17% of the BM cells 4 weeks after transplantation, whereas NC-treated cells yielded only 4.28% $hCD45^+$ cells (Fig. 7A). In addition, the proportion of $hCD34^+$ cells in the BM was increased by decHOX (decHOX, 3.05%; NC, 1.22%) (Fig. 7A). We also analyzed the lineage distributions of $hCD45^+$ cells in BM of mice that received transplants of decHOX-treated cells at 4 and 8 weeks after transplantation.

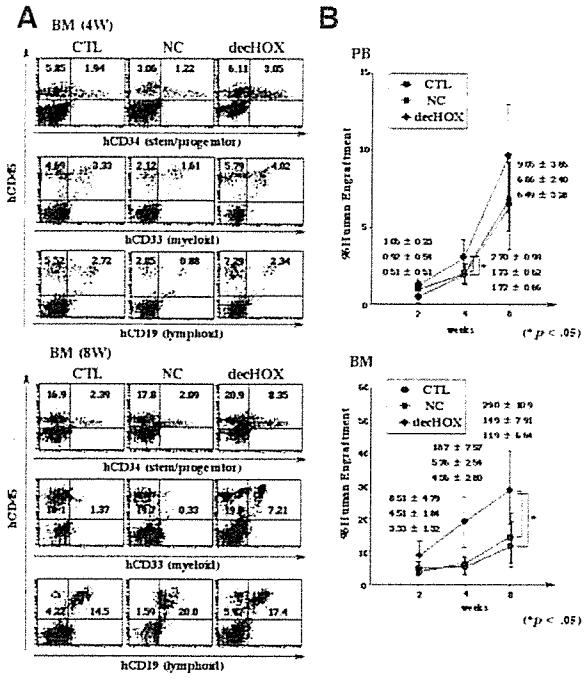

Figure 7. Xenotransplantation into nonobese diabetic/severe combined immunodeficient (NOD/SCID) mice. **(A):** A total of 2×10^4 decHOX- or NC-delivered cells were sorted and subjected to the culture for 7 days. Whole expanded cells or 2×10^4 freshly isolated $CD34^+$ cells were transplanted into 5–6-week-old NOD/SCID mice subjected to immunosuppressive treatment before and after transplantation (each group, n = 9). Four weeks after transplantation, the proportion of engrafted human cells in BM was assessed by flow cytometry with anti-hCD45-PE antibody (Ab). Four weeks and 8 weeks after transplantation, short-term repopulation abilities of the ex vivo-expanded cells were analyzed using BM and PB cells with the indicated Abs. Representative flow cytometry data obtained from BM cells are shown. **(B):** Kinetics of engraftment in PB and BM of NOD/SCID mice are indicated. Results are shown as mean ± SD (each group, n = 9). Abbreviations: BM, bone marrow; CTL, control; decHOX, decoy HOX; NC, negative control; PB, peripheral blood; PE, phycoerythrin; W, weeks.

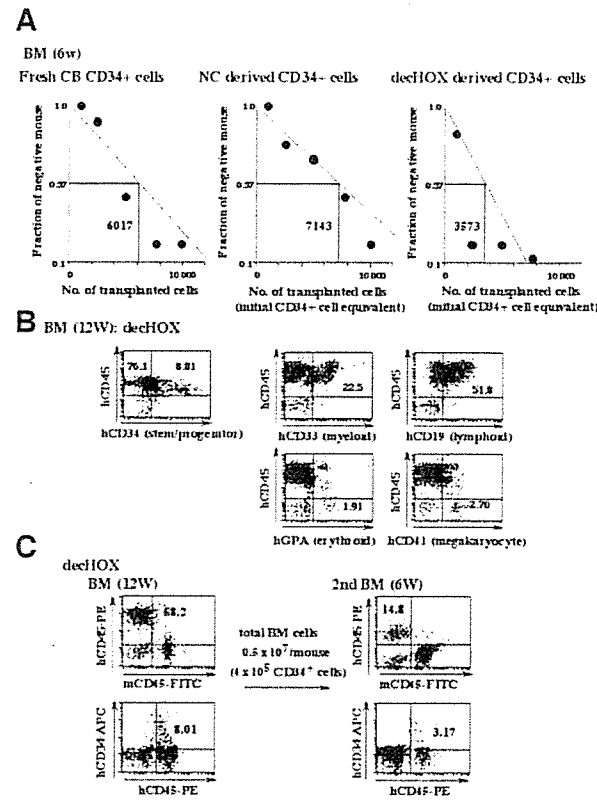

Figure 8. Long-term repopulating abilities in decHOX-delivered cells. **(A):** Frequencies of human HSCs capable of repopulating in nonobese diabetic/severe combined immunodeficient (NOD/SCID) mice in freshly isolated CB $CD34^+$ cells (n = 26), NC-treated cells (n = 29), and decHOX-treated cells (n = 23) were quantified by limiting dilution analyses. **(B):** Twelve weeks after transplantation, the long-term repopulating ability of the decHOX-treated cells was analyzed by flow cytometry using BM from NOD/SCID mouse highly reconstituted with human cells. **(C):** Twelve weeks after transplantation, BM cells were isolated from NOD/SCID mice that received transplants of decHOX-treated cells and injected into secondary recipients (n = 5). Six weeks after transplantation, the proportions of engrafted human cells in BM were assessed by flow cytometry. Representative data are shown. Abbreviations: BM, bone marrow; CB, cord blood; decHOX, decoy HOX; FITC, fluorescein isothiocyanate; hCD, human cluster of differentiation; NC, negative control; PE, phycoerythrin; W, weeks.

As shown in Figure 7A, transplanted decHOX-treated cells not only retained $CD34^+$ cells but also generated $CD33^+$ myeloid cells and $CD19^+$ B cells more effectively than CTL and NC-treated cells.

We also analyzed the kinetics of short-term repopulation in the PB and BM of recipient mice. Two weeks after transplantation, $hCD45^+$ cells were detectable in both BM and PB without significant differences in their frequencies among decHOX, NC, and CTL groups (Fig. 7B). However, at 4 weeks, the proportion of $hCD45^+$ cells in PB was significantly higher in the decHOX group than in the NC and CTL groups (decHOX, 2.70% ± 0.36%; NC, 1.73% ± 0.14%; CTL, 1.72% ± 0.16%) ($p < .05$). This result suggests that decHOX reduces the delay in engraftment associated with CB transplantation (Fig. 7B). Also, the percentage of $hCD45^+$ cells in BM was significantly higher in the decHOX group than in the CTL and NC groups at 8 weeks (decHOX, 29.0% ± 10.9%; CTL, 11.9% ± 6.64%; NC, 14.9% ± 7.91% [$p < .05$]).

Given the possibility that decHOX supports the expansion of long-term repopulating (LTR)-HSCs, we next calculated the expansion rate using a limiting dilution method. To obtain the highest possible levels of human cell engraftment, recipient mice were treated with TBI in combination with anti-asialo GM1 Ab immediately before and after transplantation (days 7, 14, 21, and 28). As shown in Figure 8A, the frequency of LTR-HSCs was calculated to be 1 in 6,017 freshly isolated CB $CD34^+$ cells and 1 in 7,143 NC-treated cells. In contrast, the frequency of LTR-HSCs in decHOX-treated cells was calculated to be 1 in 3,573. Accordingly, the expansion of LTR-HSCs by decHOX was estimated to be 2.0-fold. Furthermore, in BM highly reconstituted with decHOX-treated human cells, we detected considerable proportions of $hCD45^+CD33^+$ cells (22.5%) and $hCD45^+hCD19^+$ cells (51.8%) 12 weeks after transplantation. In addition, $hCD45^+CD34^+$ cells were an estimated 8.81% of total BM cells (Fig. 8B).

To further examine the long-term reconstituting activity of decHOX-treated cells, we performed a secondary transplantation. Twelve weeks after the first transplantation, we isolated BM cells from two mice that received transplants of decHOX-treated cells. A mixture of these cells (58.2% and 8.0% of which were $hCD45^+$ and $hCD34^+$, respectively) was transplanted into five recipients at 4.0×10^5 $hCD34^+$ cells per mouse. An apparent second engraftment was detected in the BM of 2 of 5 mice 6 weeks after the transplantation (representative data are shown in Fig. 8C). At this point, $hCD45^+$ cells were an estimated 14.8% of the total BM cells in the recipient mouse. Furthermore, approximately 20% of $hCD45^+$ cells expressed CD34 (3.17% of total BM cells). Taken together, these results indicate that CB $CD34^+$ hHSCs/HPCs expanded by decHOX reconstitute hematopoiesis more rapidly and efficiently than control cells, and these cells have long-term reconstituting abilities in NOD/SCID mice.

DISCUSSION

HOXB4-deficient mice do not exhibit obvious abnormalities in hematopoiesis except for a minor proliferative defect of HSCs detected by reconstitution assays, suggesting that HOXB4 is dispensable for normal hematopoiesis [55]. It was speculated that HOXB4 functional roles can be replaced by other HOX family members because mice lacking both HOXB4 and HOXB3 had more apparent defects in hematopoiesis than those lacking HOXB4 alone [56]. However, HOXB4 has attracted particular interest during the last few years because its gene transfer induced ~40-fold murine and ~30-fold human HSC expansion ex vivo, suggesting possible clinical applications [16, 21]. Regarding clinical use, there was an initial concern that constitutive expression of HOXB4 in HSCs might cause leukemia. This is because deregulated expression of HOXB8 was found in myeloid leukemia, and HOX family genes are sometimes involved in leukemogenic chromosomal translocations, such as t(7,11)(p15;p15), yielding NUP98-HOXA9 [57, 58]. However, HSCs expanded by HOXB4 treatment reconstituted all hematopoietic lineages in mice that received transplants mice without causing leukemia, indicating that HSCs expressing HOXB4 were regulated by the hematopoietic system [16]. To eliminate any deleterious effects caused by stable HOXB4 gene transfer, Krosl et al. tried to expand murine HSCs by delivering HOXB4 protein [20]. In that study [20], cell membrane-permeable, recombinant TAT-HOXB4 protein was added to the culture medium, inducing a fivefold net expansion of HSCs. Although TAT-HOXB4 was supposed to be delivered with high efficiency, its half-life was estimated to be only 1 hour. In addition, Amsellem et al. tried to expand human CB HSCs using HOXB4 protein [19]. They used HOXB4 protein secreted into the culture supernatant from cocultured MS-5 murine stromal cells, and this approach increased NOD/SCID mouse repopulating cells (SRCs) 2.5-fold. However, the efficiency of protein delivery was not very high, and the coculture system may not be practical for clinical applications. In contrast, our decHOX could be delivered into more than 70% of CB $CD34^+$ hHSC/HPCs and was detected in these cells even after 4 days.

Because similar decoy peptides, such as NFAT and JNK-interacting-protein-1 (JIP-1) decoy peptides were shown to be harmless at the genomic level [59, 60], decHOX may be useful for clinical applications. Furthermore, it is possible to use decHOX in combination with HOX proteins [19, 20] to further augment the activity of HOXB4. However, it should be noted that Brun et al. reported that an excessive amount of HOXB4 introduced by an adenoviral vector system inhibits self-renewal of human CB HSCs and induces myeloid differentiation [22]. Therefore, it is necessary to determine the optimal amount of HOXB4 for enforcing HSC self-renewal.

Recently, DiMartino et al. generated Pbx1-null mice, which died at embryonic day 15 or 16 due to anemia, and reported that PBX1 is required for the maintenance of definitive hematopoiesis and contributes to the mitotic amplifications of progenitor subsets [61]. However, Krosl et al. demonstrated that antisense DNA against PBX1 apparently augmented self-renewal of HSCs overexpressing HOXB4 but was not effective on normal HSCs, suggesting that PBX1 may be a negative regulator of HOXB4-mediated self-renewal of HSCs [42]. In accordance with this result, we found that decHOX could enhance cytokine-mediated self-renewal of HSCs by modifying the function of HOXB4. Furthermore, we found that decHOX restored HOXB4 activity suppressed by PBX1 without affecting DNA-binding activities. The interaction between the YPWM motif in HOX and the homeodomain in PBX1 modifies the DNA-binding affinities of the proteins and their coactivator/corepressor binding-dependent transcriptional activities, and decHOX presumably affects the latter interactions. At present, we know that decHOX can augment HOXB4-dependent transcription of c-*myc*, which we recently identified as a key regulator of HOXB4- and Notch1-mediated HSC self-renewal [49]. However, HOX-PBX complexes regulate a number of genes in HSCs both positively and negatively. Also, PBX1 shows dual (positive and negative) effects on HOX-mediated transcription according to the target genes and/or the cellular context [31, 33, 34]. Thus, further studies to identify the target genes of HOX/PBX1 in HSCs would provide useful information to facilitate decHOX-mediated ex vivo amplification of HSCs.

To date, two groups of investigators have used ex vivo-amplified CB HSCs for transplantation. Shpall et al. [5] isolated $CD34^+$ cells from CB. Forty percent of the isolated cells were expanded in medium containing SCF, G-CSF, and TPO for 10 days, and the remaining 60% were immediately transplanted or stored frozen until transplantation. After high-dose chemotherapy, 37 patients (25 adults, 12 children) received transplants of expanded $CD34^+$ cells and nonexpanded cells with a median dose of 0.99×10^7 nucleated cells per kilogram. The median time to engraftment of neutrophils (neutrophil count $> 500/\mu l$) was 28 days (range, 15–49 days) and that of platelets (platelet $> 20{,}000/\mu l$) was 106 days (range, 38–345 days). The authors of that study concluded that although the ex vivo expansion of CB cells was feasible and safe, expanded HSCs did not improve the time to engraftment in recipients [5]. In a phase I trial, Jaroscak et al. [6] transplanted CB HSCs expanded by PIXY321, FL, and EPO into 28 patients with a median dose of 2.4×10^7 nucleated cells per kilogram. They also concluded that the ex vivo expanded CB HSCs were not effective in shortening the recovery period [6]. In contrast, the present study showed that decHOX can expand short-term as well as long-term SRC, thereby shortening the delay in hematopoietic recovery, suggesting that decHOX may be an effective tool to resolve this problem. Since HSC quiescence is regulated by $p21^{waf1/cip1}$, $p16^{INK4A}$, and

$p18^{INK4C}$ and progenitor quiescence by $p27^{kip2}$ [62–66], a basic study focusing on the expression of cell cycle control molecules in decHOX-transduced cells may clarify the mechanism of decHOX-mediated rapid recovery of hematopoiesis.

In conclusion, in the present study we demonstrated that decHOX can further augment cytokine-mediated ex vivo expansion of CB HSCs and that these expanded HSCs can restore hematopoiesis more rapidly and effectively than freshly prepared CB HSCs. However, it is necessary to further optimize treatment conditions, such as the method and timing of peptide delivery. Also, to enhance the effects of decHOX, it will be useful to explore the combined effects of other signals that can support HSC self-renewal, such as SHH and Wnt. We hope that our decHOX will eventually benefit patients with hematopoietic malignancies.

ACKNOWLEDGMENTS

We are grateful to N. Takada, K. Maruyama, and M. Hirose for technical support and animal care and Y. Ikegami for laboratory management. This work was supported by grants from the Ministry of Health, Labour and Welfare of Japan (number 18790672, to N.T.), Uehara Foundation (to K.Y.), and Hovansha Foundation (to K.Y.).

DISCLOSURES

The authors indicate no potential conflicts of interest.

REFERENCES

1 Benito AI, Diaz MA, Gonzalez-Vicent M et al. Hematopoietic stem cell transplantation using umbilical cord blood progenitors: Review of current clinical results. Bone Marrow Transplant 2004;33:675–690.

2 Devine SM, Lazarus HM, Emerson SG. Clinical application of hematopoietic progenitor cell expansion: Current status and future prospects. Bone Marrow Transplant 2003;31:241–252.

3 Heike T, Nakahata T. Ex vivo expansion of hematopoietic stem cells by cytokines. Biochim Biophys Acta 2002;1592:313–321.

4 Ueda T, Tsuji K, Yoshino H et al. Expansion of human NOD/SCID-repopulating cells by stem cell factor, Flk2/Flt3 ligand, thrombopoietin, IL-6, and soluble IL-6 receptor. J Clin Invest 2000;105:1013–1021.

5 Shpall EJ, Quinones R, Giller R et al. Transplantation of ex vivo expanded cord blood. Biol Blood Marrow Transplant 2002;8:368–376.

6 Jaroscak J, Goltry K, Smith A et al. Augmentation of umbilical cord blood (UCB) transplantation with ex vivo-expanded UCB cells: Results of a phase 1 trial using the AastromReplicell System. Blood 2003;101: 5061–5067.

7 Brandon C, Eisenberg LM, Eisenberg CA. WNT signaling modulates the diversification of hematopoietic cells. Blood 2000;96:4132–4141.

8 Murdoch B, Chadwick K, Martin M et al. Wnt-5A augments repopulating capacity and primitive hematopoietic development of human blood stem cells in vivo. Proc Natl Acad Sci U S A 2003;100:3422–3427.

9 Reya T, Duncan AW, Ailles L et al. A role for Wnt signalling in self-renewal of haematopoietic stem cells. Nature 2003;423:409–414.

10 Willert K, Brown JD, Danenberg E et al. Wnt proteins are lipid-modified and can act as stem cell growth factors. Nature 2003;423:448–452.

11 Bhatia M, Bonnet D, Wu D et al. Bone morphogenetic proteins regulate the developmental program of human hematopoietic stem cells. J Exp Med 1999;189:1139–1148.

12 Bhardwaj G, Murdoch B, Wu D. Sonic hedgehog induces the proliferation of primitive human hematopoietic cells via BMP regulation. Nat Immunol 2001;2:178–180.

13 Varnum-Finney B, Xu L, Brashem-Stein C et al. Pluripotent, cytokine-dependent, hematopoietic stem cells are immortalized by constitutive Notch1 signaling. Nat Med 2000;6:1278–1281.

14 Karanu FN, Murdoch B, Gallacher L et al. The notch ligand jagged-1 represents a novel growth factor of human hematopoietic stem cells. J Exp Med 2000;192:1365–1372.

15 Ohishi K, Varnum-Finney B, Bernstein ID. Delta-1 enhances marrow and thymus repopulating ability of human CD34(+)CD38(–) cord blood cells. J Clin Invest 2002;110:1165–1174.

16 Antonchuk J, Sauvageau G, Humphries RK. HOXB4-induced expansion of adult hematopoietic stem cells ex vivo. Cell 2002;109:39–45.

17 Lessard J, Sauvageau G. Bmi-1 determines the proliferative capacity of normal and leukaemic stem cells. Nature 2003;423:255–260.

18 Park IK, Qian D, Kiel M et al. Bmi-1 is required for maintenance of adult self-renewing haematopoietic stem cells. Nature 2003;423:302–305.

19 Amsellem S, Pflumio F, Bardinet D et al. Ex vivo expansion of human hematopoietic stem cells by direct delivery of the HOXB4 homeoprotein. Nat Med 2003;9:1423–1427.

20 Krosl J, Austin P, Beslu N et al. In vitro expansion of hematopoietic stem cells by recombinant TAT-HOXB4 protein. Nat Med 2003;9:1428–1432.

21 Buske C, Feuring-Buske M, Abramavich C et al. Deregulated expression of HOXB4 enhances the primitive growth activity of human hematopoietic cells. Blood 2002;100:862–868.

22 Brun AC, Fan X, Bjornsson JM et al. Enforced adenoviral vector-mediated expression of HOXB4 in human umbilical cord blood CD34+ cells promotes myeloid differentiation but not proliferation. Mol Ther 2003;8:618–628.

23 Magli MC, Largman C, Lawrence HJ. Effects of HOX homeobox genes in blood cell differentiation. J Cell Physiol 1997;173:168–177.

24 Buske C, Humphries RK. Homeobox genes in leukemogenesis. Int J Hematol 2000;71:301–308.

25 Lawrence HJ, Helgason CD, Sauvageau G et al. Mice bearing a targeted interruption of the homeobox gene HOXA9 have defects in myeloid, erythroid, and lymphoid hematopoiesis. Blood 1997;89: 1922–1930.

26 Dorsam ST, Ferrell CM, Dorsam GP et al. The transcriptome of the leukemogenic homeoprotein HOXA9 in human hematopoietic cells. Blood 2004;103:1676–1684.

27 Crooks GM, Fuller J, Petersen D et al. Constitutive HOXA5 expression inhibits erythropoiesis and increases myelopoiesis from human hematopoietic progenitors. Blood 1999;94:519–528.

28 Bromleigh VC, Freedman LP. p21 is a transcriptional target of HOXA10 in differentiating myelomonocytic cells. Genes Dev 2000; 14:2581–2586.

29 Bjornsson JM, Andersson E, Lundstrom P et al. Proliferation of primitive myeloid progenitors can be reversibly induced by HOXA10. Blood 2001;98:3301–3308.

30 Zimmermann F, Rich IN. Mammalian homeobox B6 expression can be correlated with erythropoietin production sites and erythropoiesis during development, but not with hematopoietic or nonhematopoietic stem cell populations. Blood 1997;89:2723–2735.

31 Mann RS, Affolter M. Hox proteins meet more partners. Curr Opin Genet Dev 1998;8:423–429.

32 Pineault N, Helgason CD, Lawrence HJ et al. Differential expression of Hox, Meis1, and Pbx1 genes in primitive cells throughout murine hematopoietic ontogeny. Exp Hematol 2002;30:49–57.

33 Di Rocco G, Mavilio F, Zappavigna V. Functional dissection of a transcriptionally active, target-specific Hox-Pbx complex. EMBO J 1997;16:3644–3654.

34 Asahara H, Dutta S, Kao HY et al. Pbx-Hox heterodimers recruit coactivator-corepressor complexes in an isoform-specific manner. Mol Cell Biol 1999;19:8219–8225.

35 Saleh M, Rambaldi I, Yang XJ et al. Cell signaling switches HOX-PBX complexes from repressors to activators of transcription mediated by histone deacetylases and histone acetyltransferases. Mol Cell Biol 2000; 20:8623–8633.

36 Lu Y, Goldenberg I, Bei L et al. HoxA10 represses gene transcription in undifferentiated myeloid cells by interaction with histone deacetylase 2. J Biol Chem 2003;278:47792–47802.

37 Phelan ML, Rambaldi I, Featherstone MS. Cooperative interactions between HOX and PBX proteins mediated by a conserved peptide motif. Mol Cell Biol 1995;15:3989–3997.

38 Piper DE, Batchelor AH, Chang CP et al. Structure of a HoxB1-Pbx1 heterodimer bound to DNA: Role of the hexapeptide and a fourth homeodomain helix in complex formation. Cell 1999;96:587–597.

39 Shanmugam K, Featherstone MS, Saragovi HU. Residues flanking the HOX YPWM motif contribute to cooperative interactions with PBX. J Biol Chem 1997;272(30):19081–19087.

40 Sprules T, Green N, Featherstone M et al. Conformational changes in the PBX homeodomain and C-terminal extension upon binding DNA and HOX-derived YPWM peptides. Biochemistry 2000;39:9943–9950.

41 LaRonde-LeBlanc NA, Wolberger C. Structure of HoxA9 and Pbx1 bound to DNA: Hox hexapeptide and DNA recognition anterior to posterior. Genes Dev 2003;17:2060–2072.

42 Krosl J, Beslu N, Mayotte N et al. The competitive nature of HOXB4-transduced HSC is limited by PBX1: the generation of ultra-competitive stem cells retaining full differentiation potential. Immunity 2003;18:561–571.

43 Beslu N, Krosl J, Laurin M et al. Molecular interactions involved in HOXB4-induced activation of HSC self-renewal. Blood 2004;104: 2307–2314.

44 Tanaka H, Matsumura I, Ezoe S et al. E2F1 and c-Myc potentiate apoptosis through inhibition of NF-kappaB activity that facilitates Mn-SOD-mediated ROS elimination Mol Cell 2002;9:1017–1029.

45 Cannon MJ, Papalia GA, Navratilova I et al. Comparative analyses of a small molecule/enzyme interaction by multiple users of Biacore technology. Anal Biochem 2004;330:98–113.

46 Tajima S, Tsuji K, Ebihara Y et al. Analysis of interleukin 6 receptor and gp130 expressions and proliferative capability of human CD34+ cells. J Exp Med 1996;184:1357–1364.

47 Bhatia M, Bonnet D, Kapp U et al. Quantitative analysis reveals expansion of human hematopoietic repopulating cells after short-term ex vivo culture. J Ex Med 1997;186:619–624.

48 Wang JC, Doedens M, Dick JE. Primitive human hematopoietic cells are enriched in cord blood compared with adult bone marrow or mobilized peripheral blood as measured by the quantitative in vivo SCID-repopulating cell assay. Blood 1997;89:3919–3924.

49 Satoh Y, Matsumura I, Tanaka H et al. Roles for c-Myc in self-renewal of hematopoietic stem cells. J Biol Chem 2004;279:24986–24993.

50 Matsumura I, Kitamura T, Wakao H et al. Transcriptional regulation of the cyclin D1 promoter by STAT5: its involvement in cytokine-dependent growth of hematopoietic cells. EMBO J 1999;18:1367–1377.

51 Matsumura I, Ishikawa J, Nakajima K et al. Thrombopoietin-induced differentiation of a human megakaryoblastic leukemia cell line, CMK, involves transcriptional activation of p21(WAF1/Cip1) by STAT5. Mol Cell Biol 1997;17:2933–2943.

52 Hodel MR, Corbett AH, Hodel AE. Dissection of a nuclear localization signal. J Biol Chem 2001;276:1317–1325.

53 Gao J, Mazella J, Tseng L. Hox proteins activate the IGFBP-1 promoter and suppress the function of hPR in human endometrial cells. DNA Cell Biol 2002;21:819–825.

54 Dorrell C, Gan OI, Pereira DS et al. Expansion of human cord blood CD34(+)CD38(–) cells in ex vivo culture during retroviral transduction without a corresponding increase in SCID repopulating cell (SRC) frequency: Dissociation of SRC phenotype and function. Blood 2000;95: 102–110.

55 Brun AC, Bjornsson JM, Magnusson M et al. Hoxb4-deficient mice undergo normal hematopoietic development but exhibit a mild proliferation defect in hematopoietic stem cells. Blood 2004;103:4126–4133.

56 Björnsson JM, Larsson N, Brun AC et al. Reduced proliferative capacity of hematopoietic stem cells deficient in Hoxb3 and Hoxb4. Mol Cell Biol 2003;23:3872–3883.

57 Knoepfler PS, Sykes DB, Pasillas M et al. HoxB8 requires its Pbx-interaction motif to bl7ck differentiation of primary myeloid progenitors and of most cell line models of myeloid differentiation. Oncogene 2001;20:5440–5448.

58 Kroon E, Thorsteinsdottir U, Mayotte N et al. NUP98-HOXA9 expression in hemopoietic stem cells induces chronic and acute myeloid leukemias in mice. EMBO J 2001;20:350–361.

59 Noguchi H, Matsushita M, Okitsu et al. A new cell-permeable peptide allows successful allogeneic islet transplantation in mice. Nat Med 2004;10:305–309.

60 Kaneto H, Nakatani Y, Miyatsuka T et al. Possible novel therapy for diabetes with cell-permeable JNK-inhibitory peptide. Nat Med 2004;10: 1128–1132.

61 DiMartino JF, Selleri L, Traver D et al. The Hox cofactor and proto-oncogene Pbx1 is required for maintenance of definitive hematopoiesis in the fetal liver. Blood 2001;98:618–626.

62 Furukawa U, Kikuchi J, Nakamura M et al. Lineage-specific regulation of cell cycle control gene expression during haematopoietic cell differentiation. Br J Haematol 2000;110:663–673.

63 Cheng T, Rodrigues N, Shen H et al. Hematopoietic stem cell quiescence maintained by p21cip1/waf1. Science 2000;287:1804–1808.

64 Yuan Y, Shen H, Franklin DS et al. In vivo self-renewing divisions of haematopoietic stem cells are increased in the absence of the early G1-phase inhibitor, p18INK4C. Nat Cell Biol 2004;6:436–442.

65 Ito K, Hirao A, Arai F et al. Regulation of oxidative stress by ATM is required for self-renewal of haematopoietic stem cells. Nature 2004;431: 997–1002.

66 Cheng T, Rodrigues N, Dombkowski D et al. Stem cell repopulation efficiency but not pool size is governed by p27(kip1). Nat Med 2000;6: 1235–1240.

HOX Decoy Peptide Enhances the Ex Vivo Expansion of Human Umbilical Cord Blood CD34 + Hematopoietic Stem Cells/Hematopoietic Progenitor Cells

Hirokazu Tanaka, Itaru Matsumura, Kiminari Itoh, Asako Hatsuyama, Masayuki Shikamura, Yusuke Satoh, Toshio Heike, Tatsutoshi Nakahata and Yuzuru Kanakura

Stem Cells 2006;24;2592-2602
DOI: 10.1634/stemcells.2005-0434

International Journal of
HEMATOLOGY

Expression of CD27 on Peripheral CD4+ T-Lymphocytes Correlates with the Development of Severe Acute Graft-versus-Host Disease after Allogeneic Bone Marrow Transplantation

Hitoshi Yoshida, Tetsuo Maeda, Jun Ishikawa, Shinya Inoue, Hitomi Matsunaga, Satoru Kosugi, Masamichi Shiraga, Kenji Oritani, Yuzuru Kanakura, Yoshiaki Tomiyama

Department of Hematology and Oncology, Graduate School of Medicine, Osaka University, Osaka, Japan

Received October 31, 2005; received in revised form June 16, 2006; accepted June 29, 2006

Abstract

Allogeneic immune responses during hematopoietic reconstitution play central roles in beneficial and adverse effects after allogeneic bone marrow transplantation (allo-BMT). Appropriate regulation of the immune responses might improve the outcome of allo-BMT. However, a useful marker for monitoring allogeneic immune responses remains to be established. We enrolled 22 consecutive patients who underwent myeloablative allo-BMT between March 2002 and March 2006 and examined the relationship between CD27 expression on peripheral blood T-lymphocytes, a possible marker for naive/effector phenotypes, and clinical events, especially acute graft-versus-host disease (aGVHD). In 8 patients with aGVHD of grades II to IV, the $CD27^+/CD27^-$ ratios of $CD4^+$ (but not $CD8^+$) T-lymphocytes were significantly higher after allo-BMT, even at day 21, than the ratios in patients with aGVHD of grade 0 or I and remained high after day 21. In contrast, the ratios were low after day 21 following allo-BMT in 14 patients with aGVHD of grade 0 or I. Moreover, the clinical analysis suggested a relationship between the ratio and aGVHD grade. Thus, we showed that the $CD27^+/CD27^-$ ratio in $CD4^+$ T-lymphocytes may have value in predicting the development of severe aGVHD and may correlate with clinical symptoms of aGVHD.
Int J Hematol. 2006;84:367-376. doi: 101532/IJH97.05159

Key words: Allogeneic bone marrow transplantation; Acute GVHD; $CD4^+$ T-lymphocytes; $CD27^+/CD27^-$ ratio; Prediction

1. Introduction

Allogeneic hematopoietic stem cell transplantation (allo-SCT) has markedly improved the prognosis of patients with hematologic malignancies such as leukemia. Allogeneic immune responses during immune reconstitution after allo-SCT play central roles in beneficial and adverse effects on the outcome of allo-SCT [1]. The excellent therapeutic effects of allo-SCT on hematologic malignancies depend mainly on graft-versus-leukemia (GVL) effects [2]. The immune responses, which are generated from the differences in allogeneic antigens such as minor and/or major human leukocyte antigen (HLA) and tumor antigens, play central roles in GVL effects. In addition to the GVL effects, allogeneic immune responses after allo-SCT also play central roles in graft-versus-host disease (GVHD), which is one of the major complications after allo-SCT [3-5]. Furthermore, virus reactivation caused by the immunodeficiency created during immune reconstitution in patients who have undergone allo-SCT results in severe life-threatening infections, such as cytomegalovirus and varicella-zoster virus infections [6,7]. Thus, appropriate regulation of the allogeneic immune responses after allo-SCT would be very useful for further improving the outcome of allo-SCT. However, no useful parameters for monitoring or evaluating allogeneic immune responses after allo-SCT have been defined until now.

The expression of CD27, a member of the tumor necrosis factor receptor family, is restricted to lymphocytes [8]. With respect to T-lymphocytes, CD27 is constitutively expressed on $CD3^+$, $CD4^+$, and $CD8^+$ single-positive thymocytes. Thymic emigrants, naive T-lymphocytes, express CD45RA and CD27. Activation of mature T-lymphocytes

Correspondence and reprint requests: Hitoshi Yoshida, MD, Department of Hematology and Oncology, Graduate School of Medicine, C9, Osaka University, 2-2 Yamada-oka, Suita, Osaka, Japan; 81-6-6879-3871; fax: 81-6-6879-3879 (e-mail address: hyoshida@bldon.med.osaka-u.ac.jp).

induces strong up-regulation of CD27 expression on their cell surfaces, which can be observed only by antigen-specific stimulation, such as antigen presentation by antigen-presenting cells (APCs) [9]. In the course of activation, a soluble form of CD27 (sCD27) is produced by proteolytic cleavage at the cell surface. $CD27^-$ T-lymphocytes mainly represent the effector phenotype in both $CD4^+$ and $CD8^+$ T-lymphocytes [10].

The up-regulation of CD27 expression on naive T-lymphocytes induces these cells to express high levels of CD70, which is a ligand for CD27. Membrane expression of CD70 is also strictly dependent on antigen-receptor signaling and antigen presentation by APCs [11,12]. After initial activation by the interaction between CD28 and CD80/CD86, CD27/CD70 interactions between activated lymphocytes play important roles in the clonal expansion of T-lymphocytes and effector cell formation [12]. Several studies have suggested that CD27/CD70 interactions are primarily involved in type 1 helper T-cell immune reactions [11-13]. In allogeneic immune responses, CD27/CD70 interactions can selectively enhance the effector function of alloantigen-specific $CD8^+$ T-lymphocytes [14]. In addition, sCD27 is detectable in body fluids, and measuring sCD27 can be used to monitor local and systemic immune activation [15,16]. Thus, Lens et al proposed a model whereby CD27/CD70 interactions control the size and function of antigen-primed lymphocyte populations [8].

In conjunction with the model of Lens et al, we have hypothesized that CD27 expression on peripheral T-lymphocytes reflects an event caused by allogeneic immune responses after allo-SCT. In the present study, we monitored the expression of CD27 on $CD4^+$ or $CD8^+$ T-lymphocytes in the peripheral blood once a week after allogeneic bone marrow transplantation (allo-BMT) and found that the expression of CD27 on $CD4^+$ T-lymphocytes closely correlated with the development and severity of acute GVHD (aGVHD).

2. Patients and Methods

2.1. Patient Characteristics and Samples

We enrolled 22 consecutive patients who underwent myeloablative allo-BMT for hematologic malignancies between March 2002 and March 2006 in our hospital. As is shown in Table 1, these patients underwent allo-BMT consisting of a myeloablative conditioning regimen (total body irradiation–containing regimen, 21 patients; busulfan plus cyclophosphamide, 1 patient) and bone marrow grafting. Both bone marrow cells and peripheral blood stem cells were infused in 2 patients (unique patient numbers [UPNs] 67 and 86) because of an insufficient number of $CD34^+$ cells in the collected peripheral blood stem cells. The median age of the patients (16 men and 6 women) was 35 years (range, 17-51 years). All patients experienced hematologic malignancies (acute leukemia, 14 patients; malignant lymphoma, 3 patients; myelodysplastic syndrome, 4 patients; chronic myelogenous leukemia, 1 patient). Although all of the patients were infused with bone marrow grafts, there were HLA disparities with respect to the donor sources, as follows: sibling with HLA match, 7 patients; unrelated with HLA match, 6 patients;

Table 1.
Characteristics of the Patients Enrolled in This Study*

UPN	Age, y/Sex	Disease Status	Donor	HLA Disparity	Source	Conditioning
67	36/M	AML (refractory)	Mother	2 Loci	BM + PBSC	FLU + CY + TBI
68	51/M	ALL (2nd CR)	Unrelated	2 Loci	BM	FLU + L-PAM + TBI
69	36/F	AML (1st CR)	Unrelated	Match	BM	CY + TBI
71	44/M	NHL (refractory)	Unrelated	Match	BM	VP-16 + CY + TBI
72	48/M	AML (1st CR)	Sibling	Match	BM	CY + TBI
74	27/F	ALL (2nd relapse)	Sibling	Match	BM	CY + TBI
75	51/M	MDS (RAEB-T)	Unrelated	Match	BM	BU + CY + TBI
77	23/M	MDS (RAEB)	Unrelated	1 Locus	BM	CY + TBI
78	27/M	MDS (RAEB)	Unrelated	Match	BM	BU + CY
79	30/M	MDS (RAEB)	Mother	2 Loci	BM	CY + TBI
80	47/M	AML (1st CR)	Unrelated	Match	BM	TBI + CY
82	45/F	AML (1st relapse)	Unrelated	1 Locus	BM	BU + CY + TBI
84	34/M	ALL (1st CR)	Unrelated	Match	BM	CY + TBI
86	29/M	NHL (1st relapse)	Mother	2 Loci	BM + PBSC	BU + CY + TBI
87	44/M	AML (2nd CR)	Unrelated	1 Locus	BM	CY + TBI
89	17/F	AML (1st CR)	Sibling	Match	BM	CY + TBI
94	43/F	ALL (1st CR)	Sibling	Match	BM	CY + TBI
95	32/M	AML (1st CR)	Sibling	Match	BM	CY + TBI
96	49/F	CML (1st AP)	Unrelated	1 Locus	BM	BU + CY + TBI
103	38/M	ALL (1st CR)	Unrelated	Match	BM	CY + TBI
128	34/M	NHL (1st relapse)	Unrelated	1 Locus	BM	CY + TBI
129	48/M	ALL (1st CR)	Related	Match	BM	CY + TBI

*UPN indicates unique patient number; AML, acute myelogenous leukemia; BM, bone marrow; PBSC, peripheral blood stem cell; FLU, fludarabine; CY, cyclophosphamide; TBI, total body irradiation; ALL, acute lymphocytic leukemia; CR, complete remission; L-PAM, melphalan; NHL, non-Hodgkin's lymphoma; VP-16: etoposide; MDS, myelodysplastic syndrome; RAEB-T, refractory anemia with excess of blasts in transformation; BU, busulfan; CML, chronic myelogenous leukemia; AP, accelerated phase.

unrelated with mismatch at 1 HLA locus, 5 patients; unrelated with mismatch at 2 HLA loci, 1 patient; and mother with mismatch at 2 HLA loci, 3 patients. No severe complications were observed before allo-BMT in any patient. After informed consent was obtained from every patient, blood samples were collected at 1- or 2-week intervals starting from day 14 after allo-BMT. Observation periods ranged from 56 to 268 days after allo-BMT (mean, 105 days). Eleven healthy volunteers (6 men and 5 women) donated blood samples after they provided informed consent. This investigation was approved by the Research Ethical Committee of the Graduate School of Medicine, Osaka University.

2.2. Flow Cytometric Analysis

Fluorescein isothiocyanate (FITC)-conjugated anti-CD4 and anti-CD8 monoclonal antibodies (MoAbs) were purchased from BD Medical Systems (San Diego, CA, USA). PerCP-Cy5.5–conjugated anti-CD4 and anti-CD8 MoAbs, phycoerythrin-conjugated anti-CD27 MoAb, and FITC-conjugated anti-CD45RA MoAb were purchased from BD Pharmingen (San Diego, CA, USA). Two hundred microliters of heparinized blood were incubated with MoAbs for 30 minutes at 4°C. After 2 washes with phosphate-buffered saline (PBS), the lymphocytes were fixed, and the erythrocytes were lysed with FACS Lysing Solution (BD Immunocytometry Systems, San Jose, CA, USA). The cells were washed with PBS and stored in PBS containing 4% paraformaldehyde until the analysis. Lymphocytes, which were identified by forward and side scatter, were analyzed on a FACSort flow cytometer (BD Immunocytometry Systems) after compensation was checked.

2.3. Diagnosis of aGVHD

The classification of aGVHD was based on the diagnostic criteria of the 1994 Consensus Conference on aGVHD Grading [17], and the highest grade that occurred during the clinical course following BMT was determined.

2.4. Enzyme-Linked Immunosorbent Assay

Blood samples were obtained by venous puncture from every patient at day 21 after allo-BMT. Serum samples were collected by centrifugation and stored at –20°C until use. Serum concentrations of sCD27 were determined by an enzyme-linked immunosorbent assay kit (Sanquin Reagents/CLB, Amsterdam, the Netherlands) according to the manufacturer's instructions.

2.5. Statistics

The statistical significance of differences between the 2 groups was examined by the Mann-Whitney *U* test. Correlation was examined by evaluating the Pearson correlation coefficient.

3. Results

3.1. Expression of CD27 on Peripheral T-Lymphocytes Varies among Patients in the Early Period after Allo-BMT

To clarify the relationship between CD27 expression and clinical events associated with allo-BMT, we performed a time-course study by monitoring CD27 expression on peripheral T-lymphocytes after myeloablative allo-BMT. We analyzed the expression of CD27 on $CD4^+$ T-lymphocytes and on $CD8^+$ T-lymphocytes by 2-color flow cytometry from day 14 after BMT. Previous reports have shown that T-lymphocytes with effector phenotypes predominantly recover in the early period after allo-BMT [18,19]. In 2 patients (UPNs 72 and 79), for example (Figure 1A), the $CD4^+$ T-lymphocytes predominantly consisted of $CD27^+$ cells at day 14 after BMT. However, at day 21, peripheral T-lymphocytes predominantly expressed the $CD27^-$ effector phenotype in one of the patients (UPN 72), whereas these cells still expressed the $CD27^+$ naive phenotype in the other (UPN 79, Figure 1A). In addition to differing among patients, CD27 expression on T-lymphocytes varied among the monitoring points following BMT, even in the same patients (data not shown). To evaluate the balance between naive and effector T-lymphocytes in the peripheral blood after allo-BMT, we calculated the $CD27^+/CD27^-$ ratio for $CD4^+$ and $CD8^+$ T-lymphocytes with the formula shown in Figure 1A and analyzed the time courses of the ratio following allo-BMT (Figures 1B and 1C). In 21 of the 22 patients, $CD4^+$ T-lymphocytes predominantly consisted of $CD27^+$ cells at day 14 after BMT, leading to a high $CD27^+/CD27^-$ ratio. Compared with the $CD27^+/CD27^-$ ratio of $CD4^+$ T-lymphocytes at day 14, the ratio after day 21 dramatically decreased in 11 of 18 patients, whereas the ratio remained unchanged or increased in 8 other patients (UPNs 68, 75, 77, 78, 79, 82, 96, and 129) (Figures 1A and 1B). These results may reflect different conditions of allogeneic immune responses following allo-BMT. In contrast to $CD4^+$ T-lymphocytes, there were no clear differences among the patients after allo-BMT with respect to the $CD27^+/CD27^-$ ratio of $CD8^+$ T-lymphocytes.

3.2. A High $CD27^+/CD27^-$ Ratio for $CD4^+$ T-Lymphocytes May Correlate with the Occurrence of Severe aGVHD

To determine the relationship between the $CD27^+/CD27^-$ ratio and clinical events, we next examined the clinical features of 8 patients (UPNs 68, 75, 77, 78, 79, 82, 96, and 129) whose $CD27^+/CD27^-$ ratios of $CD4^+$ T-lymphocytes remained continuously high. Interestingly, all 8 patients developed severe aGVHD (grades II-IV), as is shown in Table 2. Moreover, in 4 of the 8 patients, steroid therapy for aGVHD was ineffective. These results suggest that a high $CD27^+/CD27^-$ ratio of $CD4^+$ T-lymphocytes may correlate with the occurrence of severe aGVHD (grades II-IV). Next, we compared the time-course analyses of $CD27^+/CD27^-$ ratios of $CD4^+$ T-lymphocytes and $CD8^+$ T-lymphocytes for the patients with no or mild aGVHD (grade 0 or I; n = 14) and those with severe aGVHD (grades II-IV; n = 8). Regarding

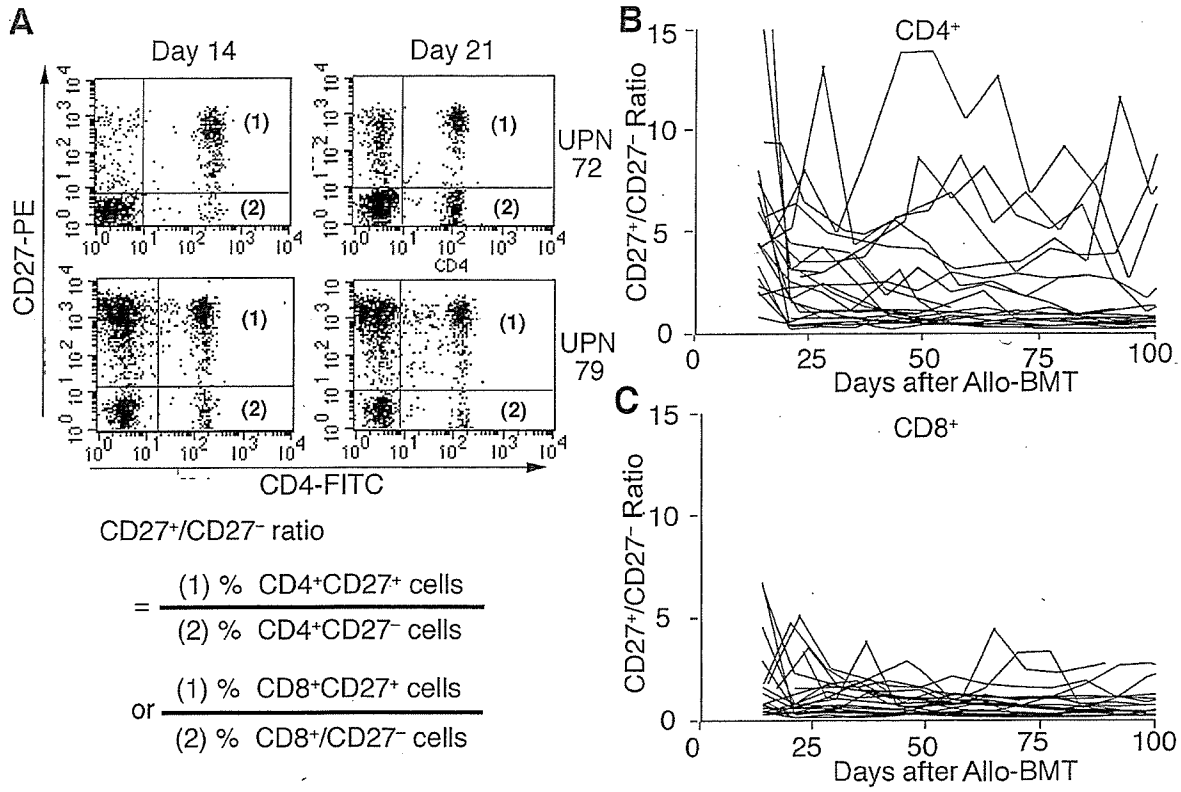

Figure 1. CD27 expression on peripheral T-lymphocytes varied among the patients who underwent myeloablative allogeneic bone marrow transplantation (allo-BMT). Representative 2-color flow cytometric analyses at day 21 after allo-BMT are shown for 2 patients (unique patient nos. [UPNs] 72 and 79) (A). The balance between naive and effector T-lymphocytes was conveniently evaluated by calculating the $CD27^+/CD27^-$ ratio for $CD4^+$ or $CD8^+$ T-lymphocytes with the formula shown in the figure. Time-course analyses of the $CD27^+/CD27^-$ ratio in $CD4^+$ (B) and $CD8^+$ (C) T-lymphocytes until day 100 after allo-BMT for all of the patients enrolled in this study. % indicates the percentage of peripheral mononuclear cells in the indicated quadrant.

$CD4^+$ T-lymphocytes, $CD27^+/CD27^-$ ratios were low at every point after day 21 in most of the patients with no or mild aGVHD (grade 0 or I) (Figure 2A), whereas $CD27^+/CD27^-$ ratios continued to be high in the patients with severe aGVHD (grades II-IV, Figure 2B). In $CD8^+$ T-lymphocytes, similar tendencies were observed. However, the differences between the 2 GVHD groups were not as clear as with $CD4^+$ T-lymphocytes (Figures 2C and 2D). In $CD4^+$ T-lymphocytes, $CD27^+/CD27^-$ ratios were significantly higher in the patients with severe aGVHD (grades II-IV) at day 21 ($P < .01$; Figure 3A) and at days 28 and 35 (data not shown). However, there was no significant difference between the 2 GVHD groups in this ratio for $CD8^+$ T-lymphocytes (Figure 3B). In the healthy volunteers, the expression of CD27 on peripheral $CD4^+$ T-lymphocytes also varied, but at a higher level than with the allo-BMT patients. In contrast, there was no apparent difference in CD27 expression on $CD8^+$ T-lymphocytes between the allo-BMT patients and the healthy volunteers. These results suggest that the expression of CD27 on $CD4^+$ T-lymphocytes in peripheral blood reflects the allogeneic immune responses and correlates with the occurrence of severe aGVHD after allo-BMT.

3.3. The $CD27^+/CD27^-$ Ratio of $CD4^+$ T-Lymphocytes at Day 21 after Allo-BMT May Have Value for Predicting the Development of Severe aGVHD

Because the $CD27^+/CD27^-$ ratios of $CD4^+$ lymphocytes were significantly high, even at day 21, in the patients who developed severe aGVHD, we examined the predictive value of the $CD27^+/CD27^-$ ratio of $CD4^+$ lymphocytes at day 21 with respect to the occurrence of severe aGVHD. Table 2 shows the maximal aGVHD grade during the clinical course, and we reevaluated the aGVHD grade from days 14 to 21 in the 8 patients with severe aGVHD. Although all 8 patients had already developed aGVHD at day 21 after allo-BMT, the aGVHD grade was I to II (Table 3). In 5 of the 8 patients (UPNs 68, 75, 77, 88, and 82), the aGVHD was ultimately upgraded to grades II to IV. Two patients with grade I aGVHD (UPNs 75 and 77)

Table 2.
Grading of Acute Graft-versus-Host Disease (aGVHD) and the Response to Therapies for aGVHD*

			aGVHD				
				Stage			
UPN	Age, y/Sex	GVHD Prophylaxis	Grade	Skin	Gut	Liver	Response to Steroid Therapy
67	36/M	FK506 + MTX + mPSL + MMF	0				
68	51/M	FK506 + MTX + MMF	IV	1	4	1	NR
69	36/F	FK506 + MTX	I	1	0	0	
71	44/M	CyA + MTX	0				
72	48/M	CyA + MTX	0				
74	27/F	CyA + MTX	0				
75	51/M	CyA + MTX	IV	2	4	0	NR†
77	23/M	CyA + MTX	IV	1	4	4	NR†
78	27/M	CyA + MTX	II	3	0	0	+
79	30/M	FK506 + MTX + mPSL	IV	1	4	0	NR†
80	47/M	CyA + MTX	I	2	0	0	+
82	45/F	CyA + MTX	II	3	0	1	+
84	34/M	CyA + MTX	I	1	0	0	+
86	29/M	FK506 + MTX + mPSL + MMF	I	1	0	0	
87	44/M	CyA + MTX	0				
89	17/F	CyA + MTX	0				
94	43/F	CyA + MTX	I	1	0	0	
95	32/M	CyA + MTX	I	1	0	0	
96	49/F	CyA + MTX	II	3	0	0	+
103	38/M	CyA + MTX	I	1	0	0	
128	34/M	FK506 + MTX + mPSL	I	1	0	0	
129	48/M	CyA + MTX	II	3	0	0	+

*UPN indicates unique patient number; FK506, tacrolimus; MTX, methotrexate; mPSL, methylprednisolone; MMF, mycophenolate mofetil; NR, no response; CyA, cyclosporin A. Shading indicates the development of aGVHD of grades II to IV.
†Infliximab was administered following ineffective steroid therapy.

and 2 patients with grade II aGVHD (UPNs 68 and 79) at day 21 finally developed grade IV aGVHD, in spite of steroid therapy. In 1 patient (UPN 78), the aGVHD grade at day 21 was maximal through the clinical course; however, the stage of skin GVHD worsened from stage 1 at day 21 to stage 3 at the maximal level. In 2 patients (UPNs 96 and 129), grade II aGVHD (skin GVHD, stage 3) had already developed at day 14 and rapidly resolved in response to steroid therapy. These results indicate the possibility that the $CD27^+/CD27^-$ ratio of $CD4^+$ T-lymphocytes at day 21 after allo-BMT has value for predicting the development of severe aGVHD.

3.4. The $CD27^+/CD27^-$ Ratio of $CD4^+$ T-Lymphocytes Responded to the Changes in aGVHD Symptoms

We further investigated the relationship between the $CD27^+/CD27^-$ ratio and the clinical course of aGVHD symptoms. Figure 4 shows schematic presentations of clinical symptoms of the patients with severe aGVHD. In 7 patients (UPNs 68, 75, 77, 78, 79, 96, and 129), the $CD27^+/CD27^-$ ratio of $CD4^+$ T-lymphocytes changed in parallel with the degree of aGVHD; that is, the $CD27^+/CD27^-$ ratio decreased when the aGVHD improved. In contrast, the ratio increased with the worsening of aGVHD symptoms. In 1 patient (UPN 82), the $CD27^+/CD27^-$ ratio increased after the occurrence of skin GVHD and eosinophilia, which is thought to correlate with GVHD [20]. These observations show that the $CD27^+/CD27^-$ ratio of $CD4^+$ T-lymphocytes may correlate with aGVHD symptoms.

3.5. The High $CD27^+/CD27^-$ Ratio of T-Lymphocytes at Day 21 after Allo-BMT Depends on a Low Number of $CD27^-$ T-Lymphocytes but Not on a High Number of $CD27^+$ T-Lymphocytes

To investigate the mechanisms responsible for the differences in the $CD27^+/CD27^-$ ratios of T-lymphocytes, we examined serum concentrations of sCD27, which reflect the conversion of CD27 expression on T-lymphocytes. At day 21, there was no significant difference in serum sCD27 concentrations between the patients with aGVHD of grade 0 or I and those with aGVHD of grades II to IV (Figure 5A), although the $CD27^+/CD27^-$ ratios of both $CD4^+$ and $CD8^+$ T-lymphocytes were moderately but significantly correlated with sCD27 levels in the sera (Figure 5B). These results suggested that the conversion from $CD27^+$ to $CD27^-$ lymphocytes might partially contribute to the $CD27^+/CD27^-$ ratio, but this conversion did not significantly differ between the 2 GVHD groups. However, the $CD27^+/CD27^-$ ratios of T-lymphocytes correlated with neither $CD27^+$ nor $CD27^-$ T-lymphocyte numbers at day 21 (data not shown). Then, we examined the numbers of $CD27^+$ and $CD27^-$ lymphocytes in the peripheral blood of the 2 GVHD groups at day 21. No significant difference was observed between the 2 groups in the absolute numbers of $CD27^+$ lymphocytes, although the numbers in both groups were markedly lower

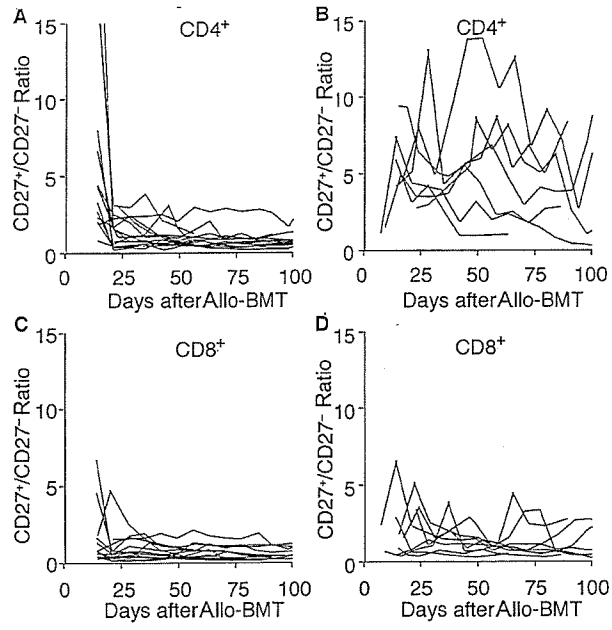

Figure 2. Changes in the time courses of the $CD27^+/CD27^-$ ratio for $CD4^+$ T-lymphocytes significantly differed between the patients with severe acute graft-versus-host disease (aGVHD) and those without severe aGVHD. Time-course analyses of the $CD27^+/CD27^-$ ratio for $CD4^+$ (A and B) and $CD8^+$ (C and D) T-lymphocytes in patients with no or mild aGVHD (A and C) or severe aGVHD (B and D) are presented. In $CD4^+$ T-lymphocytes, the time-course changes in the $CD27^+/CD27^-$ ratio were significantly different between the patients with no or mild aGVHD (A) and those with severe aGVHD (B), but not in $CD8^+$ T-lymphocytes.

than in the healthy volunteers (Figure 5C). In contrast, the absolute numbers of $CD27^-$ lymphocytes in patients with aGVHD of grades II to IV were significantly lower than the numbers in the patients with aGVHD of grade 0 or I (Figure 5D). These results suggest that the high $CD27^+/CD27^-$ ratio of $CD4^+$ T-lymphocytes in the patients with severe aGVHD results not only from a low rate of conversion from $CD27^+$ to $CD27^-$ cells but also from the trafficking of $CD27^-$ T-lymphocytes from the peripheral blood or activation-induced cell death.

3.6. The $CD4^+CD27^+$ T-Lymphocytes of the Patients Who Underwent Allo-BMT Express Low Amounts of CD45RA on Their Surfaces

We examined the expression of CD45RA, another marker for the naive phenotype, on $CD4^+CD27^+$ T-lymphocytes after allo-BMT in 3 of the patients (UPNs 103, 128, and 129). As is shown in Figure 6, approximately 10% to 30% of $CD4^+CD27^+$ T-lymphocytes expressed CD45RA on their surface during the observation period (days 14-70 after allo-BMT). Although these data were derived from only 3 patients, CD27 may not be a marker for the naive phenotype, at least in the early period after allo-BMT.

4. Discussion

Allogeneic immune responses during immune reconstitution play central roles in both beneficial and adverse effects on the outcome of allo-SCT. In this study, we found that CD27 expression on $CD4^+$ T-lymphocytes closely correlates with the development and severity of aGVHD. Moreover, a high $CD27^+/CD27^-$ ratio of $CD4^+$ T-lymphocytes in the peripheral blood at day 21 has the potential to predict the development of severe aGVHD at an early stage. Furthermore, the ratios changed in correlation with the therapy for aGVHD.

The reconstitution of T-lymphocytes in the early period after allo-BMT depends on the thymus-independent expansion of peripheral T-cells infused with the bone marrow [1]. This thymus-independent expansion is driven by antigen-dependent mechanisms. In addition, these expanded cells are primarily responsible for the success of allo-BMT through their involvement in engraftment, GVHD, the GVL effect, and virus reactivation. In this study, we analyzed the expression of CD27 and monitored the changes in the $CD27^+/CD27^-$ ratios of $CD4^+$ and $CD8^+$ T-lymphocytes, in expectation that the ratio might reflect the conditions of allogeneic immune responses after allo-BMT. In most of the patients, both $CD4^+$ and $CD8^+$ T-lymphocytes predominantly expressed CD27 at day 14 after allo-BMT. Fourteen of the 22 patients had no or mild aGVHD (grade 0 or I), and the $CD27^+/CD27^-$ ratio of the $CD4^+$ T-lymphocytes remained low in these patients beyond day 21 after BMT. Studies that have monitored the expression of CD45RA and CD45RO have demonstrated that the recovery of T-lymphocytes in the early period after allo-BMT largely consists of effector phenotype cells ($CD8^+CD45RO^+$ cells) in patients with no or mild aGVHD [18,21]. Our results are comparable with those of these previous reports, because $CD27^-$ T-lymphocytes also share the effector phenotype. In contrast, all 8 of the patients

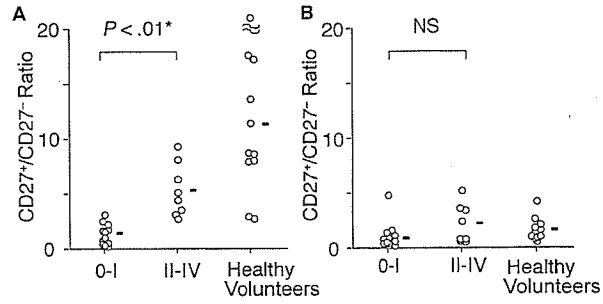

Figure 3. The $CD27^+/CD27^-$ ratio of $CD4^+$ T-lymphocytes at day 21 after allogeneic bone marrow transplantation was significantly higher in the patients with severe acute graft-versus-host disease (aGVHD). We compared the $CD27^+/CD27^-$ ratio at day 21 in $CD4^+$ T-lymphocytes (A) and $CD8^+$ T-lymphocytes (B) between the patients with no or mild aGVHD (grades 0-I) and those with severe aGVHD (grades II-IV). The higher $CD27^+/CD27^-$ ratio of $CD4^+$ T-lymphocytes in the group of patients who developed severe aGVHD, even at day 21, was statistically significant (*) by the Mann-Whitney *U* test. NS indicates not statistically significant.

Table 3.
Changes in Acute Graft-versus-Host Disease (aGVHD) Grading between Day 21 and the Point of Maximal aGVHD*

		At Day 21 after BMT				Maximal			
			Stage				Stage		
UPN	Age, y/Sex	Grade	Skin	Gut	Liver	Grade	Skin	Gut	Liver
68	51/M	II	1	0	1	IV	1	4	1
75	51/M	I	1	0	0	IV	2	4	0
77	23/M	I	1	0	0	IV	1	4	4
78	27/M	II	1	0	1	II	3	0	1
79	30/M	II	1	1	0	IV	1	4	0
82	45/F	I	1	0	0	II	3	0	0
96	49/F	II	3	0	0	II	3	0	0
129	48/M	II	3	0	0	II	3	0	0

*UPN indicates unique patient number; BMT, bone marrow transplantation.

who showed predominant expression of CD27 on $CD4^+$ T-lymphocytes (ie, a high $CD27^+/CD27^-$ ratio) developed severe aGVHD (grades II-IV). Our results suggest the existence of at least 2 different conditions of allogeneic immune responses and that the $CD27^+/CD27^-$ ratio of $CD4^+$ T-lymphocytes reflects differences in allogeneic immune responses after allo-BMT. Our results show that in addition to reflecting the different conditions of allogeneic immune responses after allo-BMT, the $CD27^+/CD27^-$ ratio of $CD4^+$ T-lymphocytes may be used to predict the occurrence of severe aGVHD, even at day 21 after allo-BMT. Moreover, the $CD27^+/CD27^-$ ratio of $CD4^+$ T-lymphocytes may correlate with changes in the severity of aGVHD. These results indicate that the $CD27^+/CD27^-$ ratio of $CD4^+$ T-lymphocytes may be a useful marker for the prevention and treatment of aGVHD in the clinical setting.

The levels of soluble Fas (sFas) and soluble interleukin 2 receptor (sIL-2R) in the sera of patients who have undergone allo-BMT have been reported to be markers for acute and chronic GVHD. In addition to the increase in sFas levels during relevant aGVHD (grades II-IV), but not in infection, significant correlations have been observed between sFas and total bilirubin levels [19]. Several reports demonstrated that serum concentrations of sIL-2R also increase in patients with aGVHD and that the peak level of sIL-2R correlates with the severity of aGVHD [20,22,23]. Moreover, sIL-2R levels decrease in response to the resolution of aGVHD symptoms. Furthermore, serum sIL-2R levels were reported to increase significantly at day 3 following transplantation, preceding the occurrence of aGVHD [22]. Our results show that the $CD27^+/CD27^-$ ratio of $CD4^+$ T-lymphocytes may also be a useful marker for the development of aGVHD, especially in combination with previously established markers. Because none of the patients enrolled in this study experienced severe infections, we could not investigate the correlation between infections and this ratio. Thus, it would be important to clarify the relationships with other complications, such as the correlation between infection and the $CD27^+/CD27^-$ ratio of $CD4^+$ T-lymphocytes.

$CD27^-$ T-lymphocytes are generated from $CD27^+$ T-lymphocytes by proteolytic cleavage after antigen-driven stimulation [24]. As a result, sCD27 is released into the serum and body fluids; consequently, sCD27 can be a useful indicator of local and systemic immune activation [15,16]. In this study, sCD27 levels were not significantly different in the sera of patients with and without severe aGVHD at day 21 after allo-BMT, although the $CD27^+/CD27^-$ ratio of total T-lymphocytes showed a moderate but significant correlation with serum sCD27 levels. These results suggest that the conversion from $CD27^+$ to $CD27^-$ cells may partially contribute to the $CD27^+/CD27^-$ ratio of T-lymphocytes. However, the absolute numbers of $CD27^-$ (but not $CD27^+$) T-lymphocytes significantly differed between the 2 GVHD groups. The apoptosis of peripheral T-lymphocytes in patients who undergo allo-BMT is increased by activation-induced cell death [25]. Apoptosis is prominent among peripheral T-lymphocytes in the early period after allo-BMT, especially in the presence of HLA disparity and aGVHD [26]. In this study, most of the patients with severe aGVHD received grafts from HLA-mismatched donors. Spectratype analyses show that the patterns observed in GVHD lesions may not follow those in the peripheral blood, demonstrating a potential impact of differential trafficking and expansion on immune reconstitution [27,28]. In this study, trafficking of activated $CD27^-$ T-lymphocytes to GVHD sites might have contributed to the significant decrease of $CD27^-$ T-lymphocytes in the patients with severe aGVHD. Thus, the $CD27^+/CD27^-$ ratio of T-lymphocytes in the peripheral blood after allo-BMT may be derived from the apoptosis or trafficking of activated T-lymphocytes as well as the conversion from $CD27^+$ cells to $CD27^-$ cells by antigen-driven stimulation.

Recently, the effector phenotype of T-lymphocytes was reported not to cause GVHD, whereas the naive phenotype of $CD4^+$ T-lymphocytes was found to cause severe aGVHD in a murine experimental model of GVHD [29,30]. Our findings that the proportion of $CD27^+CD4^+$ T-lymphocytes (ie, naive $CD4^+$ T-lymphocytes) was significantly and prominently high among patients with severe aGVHD (grades II-IV) possibly reflects the results of murine models in a human clinical setting, although the analyses were performed with peripheral blood T-lymphocytes. However, the low expression of CD45RA on $CD4^+CD27^+$ T-lymphocytes in 3 of the patients leads to the speculation that CD27 expression indicates an activation marker but not a naive phenotype.

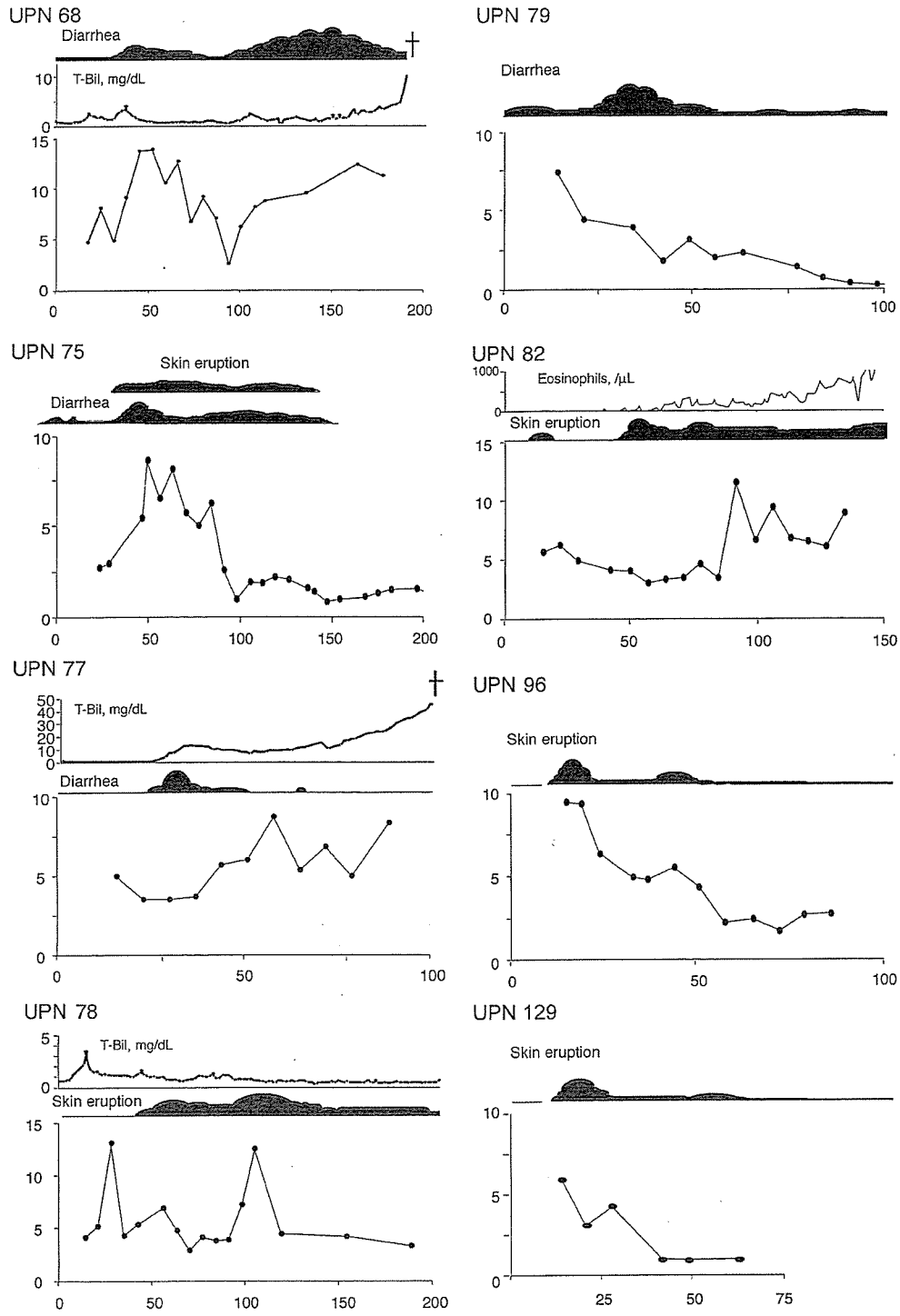

Figure 4. The $CD27^+/CD27^-$ ratio of $CD4^+$ T-lymphocytes responded to changes in acute graft-versus-host disease (aGVHD) symptoms. Schematic presentations of the clinical course of aGVHD symptoms for the patients with severe aGVHD and the $CD27^+/CD27^-$ratio of $CD4^+$ T-lymphocytes are shown (unique patient nos. [UPNs] 68, 75, 77, 78, 79, 82, 96, and 129). The $CD27^+/CD27^-$ ratio of $CD4^+$ T-lymphocytes responded according to the worsening or improvement of aGVHD symptoms. The x-axis represents days after allogeneic bone marrow transplantation; the y-axis represents the $CD27^+/CD27^-$ ratio of $CD4^+$ T-lymphocytes unless otherwise indicated. T-Bil indicates total bilirubin; a cross indicates patient death.

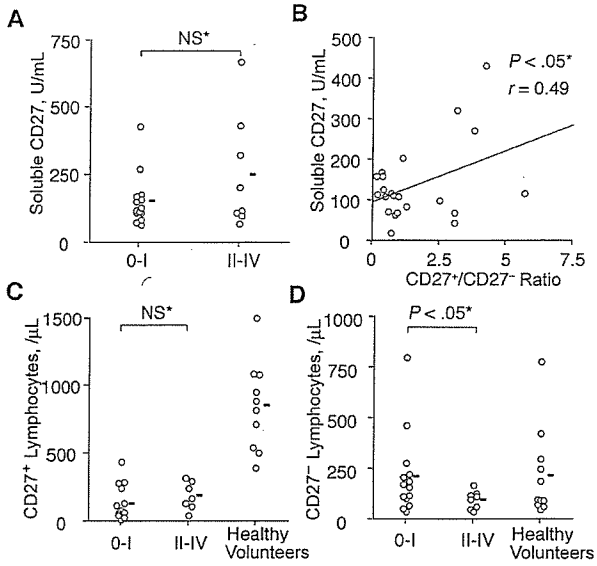

Figure 5. A high $CD27^+/CD27^-$ ratio of peripheral T-lymphocytes at day 21 after allogeneic bone marrow transplantation depended on a low amount of $CD27^-$ T-lymphocytes. Differences in soluble CD27 (sCD27) levels in sera at day 21 between the patients with no or mild aGVHD (grades 0-I) and those with severe aGVHD (grades II-IV) (A) were not significantly different (NS). A moderate but statistically significant (**) correlation (Pearson correlation coefficient) was observed between serum concentrations of sCD27 and the $CD27^+/CD27^-$ ratios of both $CD4^+$ and $CD8^-$ T-lymphocytes (B). The absolute number of peripheral $CD27^-$ T-lymphocytes at day 21 was significantly lower in the patients with severe aGVHD than in those with no or mild aGVHD (D), whereas the absolute numbers of $CD27^+$ T-lymphocytes for the 2 GVHD groups were not significantly different (C). A statistically significant difference between the 2 groups according to the Mann-Whitney *U* test is indicated (*).

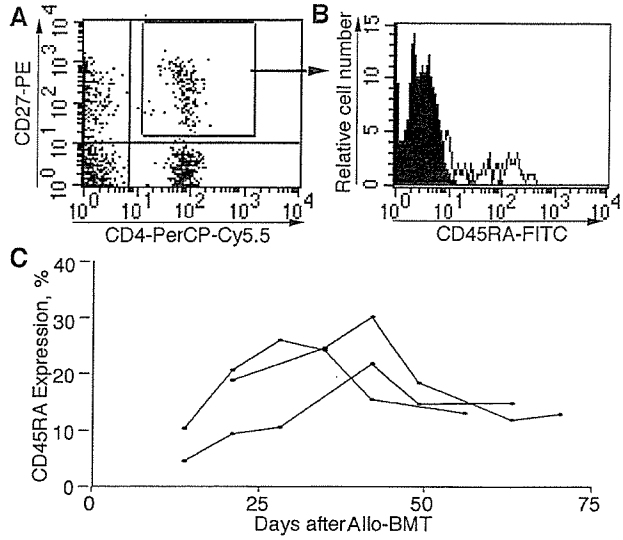

Figure 6. The $CD4^+CD27^+$ T-lymphocytes of patients who underwent allogeneic bone marrow transplantation (allo-BMT) expressed a low amount of CD45RA on their surfaces. We examined 3 patients (unique patient nos. [UPN] 103, 128, and 129) with respect to the expression of CD45RA on $CD4^+CD27^+$ T-lymphocytes after allo-BMT. Representative data (UPN 128) from 3-color flow cytometric analyses are shown in (A) and (B). The shaded and open histograms show the data for isotype-matched immunoglobulin G and anti-CD45RA monoclonal antibody, respectively. Time-course analyses of the expression of CD45RA on $CD4^+CD27^+$ T-lymphocytes after allo-BMT are shown in (C). PE indicates phycoerythrin; FITC, fluorescein isothiocyanate.

In this study, the $CD27^+/CD27^-$ ratio of $CD4^+$ T-lymphocytes, but not $CD8^+$ T-lymphocytes, closely correlated with the development and severity of aGVHD. Both $CD4^+$ and $CD8^+$ T-lymphocytes can contribute to the development of aGVHD, which is derived from the disparity of the major histocompatibility complex (MHC) and minor histocompatibility antigens. $CD4^+$ T-lymphocytes alone mediate GVHD when the disparity in the MHC exists only at class II loci, whereas $CD8^+$ T-lymphocytes are responsible for GVHD caused by only an MHC class I disparity. MHC class II molecules are primarily limited to APCs and are aberrantly expressed on the cells of nonhematopoietic tissues during GVHD [31,32], whereas MHC class I molecules are present on virtually all nucleated cells. In addition to alloantigen presentation to donor T-lymphocytes by APCs, MHC class II molecules aberrantly expressed on epithelial cells seem to be critical for the development of aGVHD [31-33]. Recently, $CD4^+$ T-cells were reported to play important roles in the pathogenesis of aGVHD in a murine aGVHD model using irradiated hosts, not only by direct attack but also via modulation of alloreactive $CD8^+$ T-cells [34,35]. These facts may indicate one of the reasons that the $CD27^+/CD27^-$ ratio in $CD4^+$ T-lymphocytes, but not $CD8^+$ T-lymphocytes, can be used to monitor aGVHD. The requirement of multiple markers to distinguish a subset of $CD8^+$ T-lymphocytes may also contribute to the differences in the $CD27^+/CD27^-$ ratio between $CD4^+$ and $CD8^+$ T-lymphocytes [36].

Allogeneic immune responses play critical roles in the pathogenesis of complications such as aGVHD and infections. The control of these complications can further improve the outcome of allo-SCT for hematologic diseases. In this study, we have demonstrated that the $CD27^+/CD27^-$ ratio of $CD4^+$ T-lymphocytes of the peripheral blood closely correlates with the development and severity of aGVHD, even though the research subjects were limited to 22 patients with heterogeneous backgrounds who underwent myeloablative allo-BMT. Expression of CD27 on peripheral $CD4^+$ T-lymphocytes appears to reflect allogeneic immune responses after allo-BMT and may be a useful marker for aGVHD.

Acknowledgments

This work was supported in part by a grant from the Ministry of Education and Science. We thank Ms. Natsu Iwamoto, Ms. Sonoe Shima, and Ms. Tomoko Okura for their preparation of blood samples and secretarial assistance.